UNIVERSIDAD SAN FRANCISCO DE QUITO USFQ

COLEGIO DE CIENCIAS E INGENIERÍAS

LIGNOCELLULOSE CELL WALL FRACTIONATION OF BREWER´S SPENT GRAINS WITH A DEEP EUTECTIC SOLVENT FOR CELLULOSE AND XYLAN ISOLATION AND CHARACTERIZATION

Proyecto de Investigación

JUAN BERNARDO GUERRERO PÁEZ

INGENIERÍA QUÍMICA

**Trabajo de titulación presentado como requisito
para la obtención del título de
Ingeniero Químico**

Quito, 21 de mayo de 2019

UNIVERSIDAD SAN FRANCISCO DE QUITO USFQ

COLEGIO DE CIENCIAS E INGENIERÍAS

HOJA DE CALIFICACIÓN
DE TRABAJO DE TITULACIÓN

LIGNOCELLULOSE CELL WALL FRACTIONATION OF BREWER´S SPENT GRAINS WITH A DEEP EUTECTIC SOLVENT FOR CELLULOSE AND XYLAN ISOLATION AND CHARACTERIZATION

JUAN BERNARDO GUERRERO PÁEZ

Calificación:

Nombre del profesor, Título académico

Lourdes Magdalena Orejuela Escobar, PhD

Firma del profesor

_____

Quito, 21 de mayo de 2019

Derechos de Autor

Por medio del presente documento certifico que he leído todas las Políticas y Manuales de la Universidad San Francisco de Quito USFQ, incluyendo la Política de Propiedad Intelectual USFQ, y estoy de acuerdo con su contenido, por lo que los derechos de propiedad intelectual del presente trabajo quedan sujetos a lo dispuesto en esas Políticas.

Asimismo, autorizo a la USFQ para que realice la digitalización y publicación de este trabajo en el repositorio virtual, de conformidad a lo dispuesto en el Art. 144 de la Ley Orgánica de Educación Superior.

Firma del estudiante: _____

Nombres y apellidos: Juan Bernardo Guerrero Páez

Código: 00116134

Cédula de Identidad: 1718721069

Lugar y fecha: Quito, 21 de mayo de 2019

RESUMEN

En el presente estudio se partió del pretratamiento de afrecho de cebada con solventes eutécticos profundos a base cloruro de colina (ClCh) y glicerol (gly) y con autohidrólisis para el aislamiento de xilano y celulosa a dos temperaturas diferentes: 105 y 125   . Los dos pretratamientos fueron realizados para comparar la eficiencia de extracción del primero vs. el segundo. Seguido, se realizó extracción alcalina y blanqueamiento con el objetivo de separar la hemicelulosa y remover la lignina residual. Posteriormente, se retiró el xilano de la hemicelulosa precipitándolo con metanol al 94% que también se blanqueó y se secaron los biopolímeros obtenidos. Finalmente, se realizó la caracterización de los productos a través del espectrómetro infrarrojo con trasformada de Fourier, el difractómetro de rayos X, la calorimetría diferencial, el análisis termogravimétrico y el microscopio electrónico de barrido. Este estudio permitió definir el uso de los solventes eutécticos profundos como una herramienta más practica para la obtención y caracterización de biopolímeros. Por otra parte, los análisis permiten concluir que se obtienen biopolímeros con baja cristalinidad y apropiados para la funcionalización de grupos hidróxido superficiales. Además, se comprueba que las muestras tienen propiedades térmicas superiores y una morfología irregular.

Palabras Clave: fraccionamiento de la biomasa, afrecho de cebada cervecera, solventes eutécticos profundos (SEP), autohidrólisis, xilano, celulosa.

ABSTRACT

In this study, isolation of cellulose and xylan from brewer´s spent grains (BSG) biomass using a mixture of choline chloride (ChCl) and glycerol deep eutectic solvents (DES) and autohydrolysis were performed in order to fractionate the lignocellulosic cell wall. The two experiments were done at mild temperatures (105 and 125) as comparative studies to analyze their polymers extraction efficiency and biopolymers' quality. After pretreatments, alkali extraction was carried out to remove hemicellulose and lignin and obtain an unbleached cellulose fraction. Later, xylan was isolated from hemicellulose with 94% methanol and bleached, along with cellulose fraction, with sodium hypoclorite (5%). Final biopolymers obtained were dried. Mass balances were performed to evaluate the pretreatment extraction efficiency. The two polymeric fractions obtained were analyzed with Fourier Transformed Infrared Spectroscopy (FTIR) to characterize the materials through identification of the main functional groups. Moreover, characterization of cellulose samples was performed by determining crystallinity, thermal stability properties and morphology using techniques such as X-ray Diffraction Method (XRD), Thermogravimetry Analysis (TGA), Differential Scanning Calorimetry analysis (DSC) and Scanning Electron Microscopy analysis (SEM), respectively. As a result, FTIR confirm the nature of species to be cellulose and xylan with residual hemicellulose and lignin. XRD allowed to identify cellulose as type I (native) for samples treated with ChCl/glycerol DES (1:2) deep eutectic solvent at $105^{o}C$ and samples subjected to autohydrolysis at $105^{o}C$ and $125^{o}C$. Thermal analysis showed that samples had typical cellulose and xylan degradation temperatures. Finally, SEM image analyses allowed to identify some individual cellulose microcrystals as well as agglomerated cellulose fibrils. These two pretreatments showed the possibility to isolate cellulose and microcrystalline cellulose from BSG biomass with deep eutectic solvents. Further studies of physico-mechanical tests would allow to determine potential industrial applications as micro/nanocomposites. Additionally, cellulose/xylan functionalization would lead to cellulose/xylan derivatives with interesting applications in food, pharmaceutical, cosmetic, biomedical, pulp and paper, packaging and textile industries.

Key words: biomass fractionation, brewers spent grains (BSG), deep eutectic solvents (DES), autohydrolysis, xylan, cellulose.

Table of Contents

INTRODUCTION

From a global point of view, societies through the world have the arising concern of solving social and environmental issues that affect everyone´s life regarding contamination and the use of fossil fuels. In this sense, it results imperative to reutilize agro-industrial sub-products from agriculture and specially food and beverage industry to produce high valued chemicals, and essentially avoid further contamination from these residues that have rich organic matter composition and may alter ecosystems (Alexandre, Mathias, Sérvulo, Cammarota, & de Mello, 2015). In this context, by-products generated from the brewing industry that include barley, hops and yeast, have great potential to be reused due its worldwide availability (Mussatto, 2014). This study attempts to assess the effect of ChCl/glycerol DES on BSG at two different temperatures and compare its efficiency to autohydrolysis pretreatment at the same experiment conditions as well as to characterize the obtained biopolymers.

Brewer's Spent Grains (BSG)

BSG are generated worldwide with an annual output of 39 million tons constituting breweries' main by-product. Essentially, it is composed of barley or wheat husk produced after polysaccharide extraction (Lynch, Steffen, & Arendt, 2016) and contains protein, polysaccharides and lignin. BSG main application is as animal food supplements due to its high nutritional value, however, since it is rich in polysaccharide as well as phenolic compounds, this beverage industry by-product has great potential for revalorization into high valued compounds (Refer to Annex 1 for BSG composition reference).

Ecuador is a farmland country with a great potential for biomass reutilization due to its agriculturally based economy that generates all types of plant residues. Moreover, there is a high availability of BSG since beer is the most consumed alcoholic beverage in the country (El Comercio, 2016). Despite its main use in animal diet, companies' interest in revalorizing their residues is high to obtain valued derived products from its main chemical components such as proteins, cellulose, hemicellulose and lignin that can potentially be of great interest to other industries such as cosmetics, craft pulping, textiles, food and agricultural packaging and pharmaceutics (Reubroycharoen et al., 2018). This would increase the brewery's competitiveness and productivity and would allow to diversify production. However, BSG biomass needs to go through biorefining processes to assess revalorization possibilities.

BSG Biomass Fractionation and Biorefineries

Biorefineries are biomass processing plants whose purpose is to reuse organic residues from a biotechnological point of view to obtain high value products according to the industry needs. Their main objective is to substitute large scale oil plants derived products that are the source of the most materials used today with bio-based ones (Elmekawy, Diels, De Wever, & Pant, 2013). This can be done by transforming biomass organic waste coming from forest, agriculture, agroindustry and food industry to produce traditionally oil derived products such as materials, plastics, chemicals, energy and food supplements (Brányik et al., 2019; Charpentier, 2016; Procentese et al., 2018)

The most industrially and economically relevant materials that can be recovered from BSG biomass are bioactive compounds which are extractable with solvents and are of great interest for pharmaceutics, food industry and cosmetics, For instance ferulic acid is related to cancer risk reducing properties (Moreira, Morais, Barros, Delerue-Matos, & Guido, 2012). Extractive free BSG biomass can undergo cell wall fractionation and produce a variety of chemical compounds and biofuels. Sugars from holocellulose (polysaccharide), especially cellulose, can be isolated from BSG biomass and used to produce bio-based chemicals and materials as well as bioethanol (Mussatto, 2014). Bio-alcohol is made by chemically or thermally pretreating biomass and then performing saccharification with cellulases and xylanases followed by fermentation with microorganisms to produce ethanol (Paschos, Xiros, & Christakopoulos, 2015; Wilkinson, Smart, James, & Cook, 2017). Another important chemical that can be obtained from BSG biomass, due to its high hemicellulose content is xylan, which can be used as a biofilm for food packaging and other industrial applications. Additionally, depolymerizing xylan into xylose (C_5 sugar), to ferment with Candida guilliermondii is used to produce xylitol (Mussatto & Roberto, 2005).

Additionally, lignin's oligomers and/or monomers can be isolated, purified and characterized to interesting aromatic compounds that are applicable as adhesives, resins, emulsifiers, dispersants for chemical industry and even as pharmaceutics. For example, low-molecular-weight lignins such as vanillin and syringaldehyde are valuable compounds used in cosmetics and medicine (Q. Chen et al., 2018; Hassan, Williams, & Jaiswal, 2019; Ma et al., 2016; Orejuela, Renneckar, Goodell, Frazier, & Edgar, 2017). Lately, lignin oligomers have been

modified into functionalized aromatic compounds (Diels, 2019). Moreover, cellulose, micro/nanocellulose, hemicellulose and lignin structural biopolymers isolated form lignocellulosic biomass can be included into biomaterials (Adnan et al., 2016) with advanced physicochemical properties (N. Lin & Dufresne, 2014)(R. D. Singh, Banerjee, Sasmal, Muir, & Arora, 2018).

However, prior to this, biomass needs to undergo one or several pretreatment processes to enhance cellulose accessibility and fight biomass recalcitrant nature, which does not allow chemicals or biological organisms to act on specific parts of the cellular wall structure that has crosslinked conformation that protects cellulose (C. W. Zhang, Xia, & Ma, 2016).

Lignocellulose Plant Cell Wall

Plants and algae cell walls are divided in two types: primary and secondary. While the first type is mainly composed of cellulose, hemicellulose, pectin and proteins, the second one develops when plant reaches maturity and is mostly cellulose (30-60), hemicellulose (20-40) and lignin (15-25%). However, the composition depend on the source (Wertz, Deleu, Coppé, 2017). Cellulose, the main cell wall component, is a polysaccharide formed of glucan monomers (which are 6 carbon sugars) linked up by $\beta - 1,4$ glucoside bonds. Interestingly, it is the most abundant biopolymer on earth with total annual synthesis of 100 billion tons a year (Ambavaram, Krishnan, Trijatmiko, & Pereira, 2010). There are 4 different polymorphs of cellulose which are cellulose I, II, III and IV. Cellulose I and II are the most studied and differ in that type I has parallel crystalline chains while type II has anti-parallel chains (Yue, 2011). Moreover, it is an aggregation of chains that form crystalline an amorphous structures depending on how ordered the sections are (Brown, 1999). These aggregations or microfibrils build up to form the core structure of a plant and give its strength.

Hemicellulose is referred as a crosslinking branched polymer that binds tightly to cellulose by hydrogen bonding interactions giving strength to the plant (Scheller & Ulvskov, 2010). It is conformed of a polymer matrix that include xyloglucans, xylans, arabinoxylans, mannans and glucommans which in return are built of 5 and 6 carbon monomers such as glucose, xylose, galactose and arabinose (Wertz, Deleu, Coppé, 2017). Furthermore, the term hemicellulose is archaically used for all low molecular weight polymers that dissolve in alkali solutions. On the other hand, xylan is the most common hemicellulose in nature that consist of

β_{-D-}xylopyranosyl units (xylose) linked by $\beta - 1,4$ glucosidic bonds (Naidu, Hlangothi, & John, 2018). Xylan backbone might have other fundamental sugars in its branching giving rise to several subcategories like: arabinoxylan, glucuronoxylan and arabinoglucuronoxylans. Moreover, homoxylan, namely xylan, consist only of xylose and can be linear or branched (Chakdar et al., 2016).

Lignin is a generic name for a large number of aromatic polymers condensed from precursors monolignols such as p-coumaryl alcohol, coniferyl alcohol and sinapyl alcohol (The three main monolignols can be seen in annex 2). Precursors form the fundamental lignins which are called p-hydroxyphenyl (H), guaiacyl (G) and syringil (S) (Ralph, 1998). Lignin is the only naturally synthetized polymer with an aromatic backbone, and it determines the rigidity factor in a plant as it is deeply crosslinked with cellulose and hemicellulose, as well as provides hydrophobicity to the structure. An illustration of the main plant components and their building block can be observed in Annex 3.

Cell walls are classified according to the six-representative group of plants which are: non-grass angiosperms, grasses, gymnosperms, leptosporangiates and in eusporangiates (Wertz, Deleu, Coppée, & Richel, 2017). Brewery Spent Grain cell wall is part of the grass group that is characterized by high presence of arabinoxylans and mixed linked glucans making it a great source of xylose and glucose (Carpita, 1996).

Lignocellulose Biomass Pretreatments

The importance of pretreatment methods has been widely recognized in biomass revalorization process to achieve high efficiency (Galia et al., 2015). The main objectives of pretreatments are to 1) remove lignin and hemicellulose (or rather separate them for further use); 2) promote the formation of sugars and valuable derivate chemicals such as hydroxymethylfurfural; and, 3) avoid the formation of inhibitory byproducts (Y. Sun et al., 2016). Moreover, the processes can be tuned (Galia et al., 2015) to increase the cellulose crystallinity, recover lignin or synthetize nano-structures.

In this sense, the first methods developed were based on the craft pulping industry, that developed processes based on the use of organic solvents that demonstrated to effectively isolate cellulose, however they were dangerous and threaten the environment due to its "acute and

chronic toxicity, carcinogenicity, ecological toxicity and non-biodegradability" (Khandelwal, Tailor, & Kumar, 2016). From then on, a variety of different approaches have been taken in order to pretreat biomass, investigating in the power of thermal heat, chemicals and microorganism on recalcitrance. To resume, the main methods developed and used up to date are described in Figure 1.
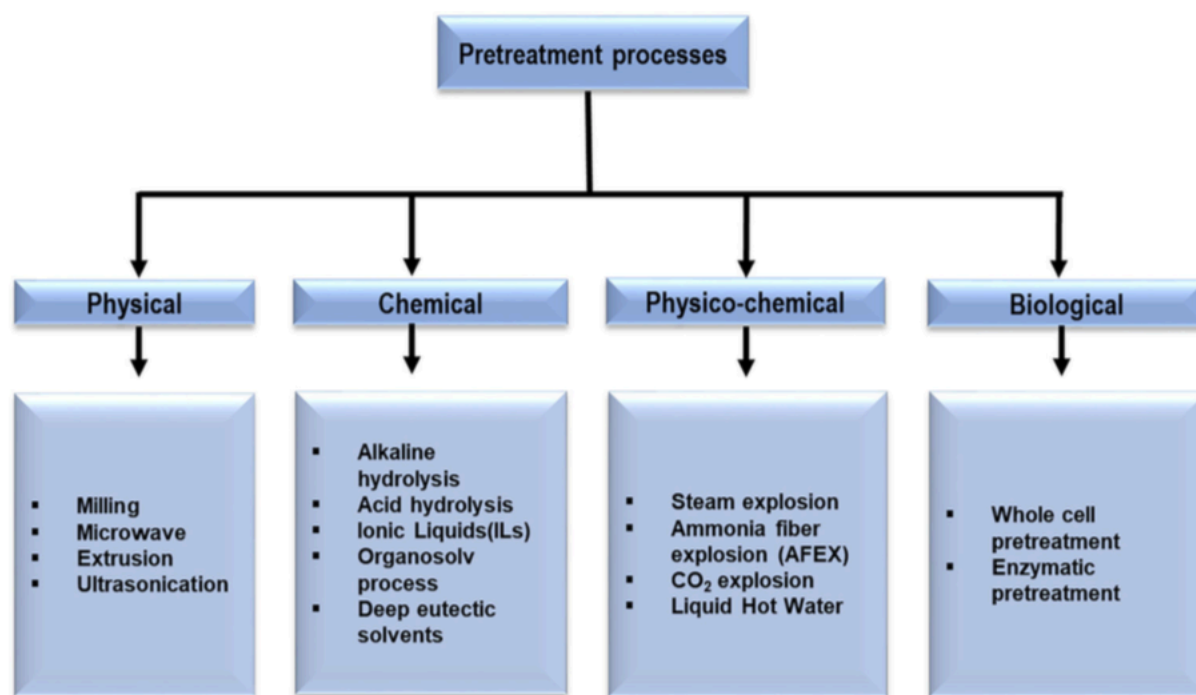
Figure 1: Lignocellulosic Biomass Pretreatment methods. Taken from (Baruah et al., 2018) under fair use

Physical pretreatments are a requirement prior to cell wall attack in order to increase accessibility to cellulose, decrease polymerization and cellulose crystallinity (Rajendran, Drielak, Varma, Muthusamy, & Kumar, 2017). Wet-milling disk is a relevant pretreatment to this research that has the purpose of reducing the particle size and increase the contact area exposed to any chemical, therefore decreasing the biomass recalcitrance (Hideno et al., 2009). Another important physical pretreatment is ultrasonication which utilizes ultrasound radiation to promote cavitation and strong shear stress in the complex lignocellulosic structure. It can be used to extract components and produce nanocellulose (Baruah et al., 2018).

Among physico-chemical pretreatments, autohydrolysis (sometimes also called steam explosions or liquid hot water) stands out like an efficient low-cost process where cell wall is

broken by heating biomass in water at different temperature and pressure ranges. In this process, hydronium ions are generated at high temperatures promoting cleavage of cellulose hemicellulose and lignin which at the same time generates acidic compounds like formic, acetic, levulinic, uronic and phenolic acids from polymers saccharification. The mentioned compounds would promote further depolymerization avoiding in this way the use of additional mineral acids. (Galia et al., 2015). Moreover, since the only chemical used is water, relevant advantages have been recognized in this process such as low by-product generation, low equipment corrosion related to neutral pH and no neutralization or purification cost (Lorente et al., 2015). Equally important, hemicellulose oligosaccharides and lignin acids are majorly preserved. A major drawback is that at very low pH values sugar are degraded into hydroxymethylfurfural HMF (V. Singh, Parsons, & Pettigrew, 2007).

Regarding the use of chemicals, some harsh ones (acids and bases) are used in the pulp and paper industry, while others are greener and biological based (Z. Chen & Wan, 2018). Therefore, friendlier pretreatment methods are essential for a healthy development of biorefineries. Several researches have focused on the development of green technologies for biomass processing and conversion (A. P Abbott, Boothby, Capper, Davies, & Rasheed, 2004; Dai, Spronsen, & Witkamp, 2013; Durand, Lecomte, & Villeneuve, 2016; Francisco, Van Den Bruinhorst, & Kroon, 2012; Meléndez-Martínez, Vicario, & Heredia, 2007; Vigier, Chatel, & Jérôme, 2015) dabbling in the use of solvents such as ionic liquids, and deep eutectic solvents (DESs). In this sense, DESs have arose like one of the most promising environmentally and human friendly solvents with high affinity for lignin extraction (Andrew P. Abbott et al., 2011; Lei et al., 2017; Radošević et al., 2015).

Deep Eutectic Solvents

Among the chemical pretreatments, organosolv was developed in order to decrease the use of harsh chemicals and also because it allows the recovery of three different streams: cellulose, hemicellulose and lignin after the pretreatment and the filtration processes. Main organic solvents used are formic acid, acetic acid, acetone, methanol, ethanol, ethylenglycol and other alcohols (Matsutani, Harada, Ozaki, & Takaoka, 1993). However, these solvents are volatile, expensive, toxic and hazardous (Z. Zhang, Harrison, Rackemann, Doherty, & O'Hara, 2016). To overcome these drawbacks, ionic liquids emerged as a new type of non-volatile and highly selective solvents, which represents a greener approach in biorefinery settings (Klein

Marcuschamer, Simmons, & Blanch, 2011). Unfortunately, ionic liquids have been proved not to be so environmentally friendly solvents, besides they are costly and most of the times difficult to handle. Therefore, deep eutectic solvents were developed as the new green solvents for lignocellulosic biomass processing (Andrew P. Abbott et al., 2011; Bubalo, Senka Vidovic, Redovnikovic, & Joki, 2018; Mamilla, Novak, Grilc, & Likozar, 2019; Vigier et al., 2015).

There are several types of DES beginning by type I which is formed when a quaternary ammonium salt mixes with metal halides. Type II are created when the same salts interacts with hydrated halides while type III is the mix of as the ammonium salt acts as a HBA to a HBD specie (Andrew P. Abbott, Barron, Ryder, & Wilson, 2007). Deep Eutectic Solvents (DESs) type III are mixtures of two or more components defined as a hydrogen bond donor (HBD) and a hydrogen bond acceptor (HBA) (A. P Abbott et al., 2004). The system has a lower melting point and lower lattice energy than its individual components due to the molecular bond interaction (Liimatainen et al., 2016). Moreover, they show several advantages over traditional solvents such as low vapor pressure (as ionic liquid) inexpensive cost of raw materials, low to moderate toxicity and biodegradability contributing to its environmental friendliness (Craveiro et al., 2016). From a practical point of view, this type of solvent offer advantages such as easiness to dissolve in organic solvents, tolerance to water, adjustable acidity, dissolution agents and biomass fractionation (Orejuela et al., 2017).

DESs have been prepared extensively with the use of choline chloride (ChCl) as a (HBA) which is a non-expensive, human and environmentally friendly quaternary ammonium (Andrew P. Abbott et al., 2006)(Andrew P. Abbott et al., 2011)(Wolfson, Dlugy, Shotland, & Tavor, 2009). This chemical is versatile and can form solutions with several HBDs such as: urea, renewable carboxylic acids (citric or amino acids) or renewable polyols (glycerol or carbohydrates) (Liimatainen et al., 2016). DES and NADES (natural deep eutectic solvents) are present around the membrane cellular wall and are involved in biosynthesis, solubilization and storage of compounds in cells. Moreover, they can solubilize valuable extractives that can be added to food (Dai, Verpoorte, & Choi, 2014).

Moreover, ChCl and glycerol, also known as glyceline (Orejuela et al., 2017) system has been widely studied to better understand its properties (Lei et al., 2017)(Loow et al., 2017)(Xing,

Xu, Dong, Han, & Ni, 2018). Simply by adding 33% of the ammonium salt to glycerol its viscosity dramatically decreased. The mixture becomes a liquid, after mixing at 80 , with extremely lower melting point of -40 that differs greatly from the original (17.5) (Andrew P. Abbott et al., 2011). ChCl makes the OH groups in glycerol available to react by disrupting natural occurring hydrogen bonds. The schematic molecular interaction is shown below:
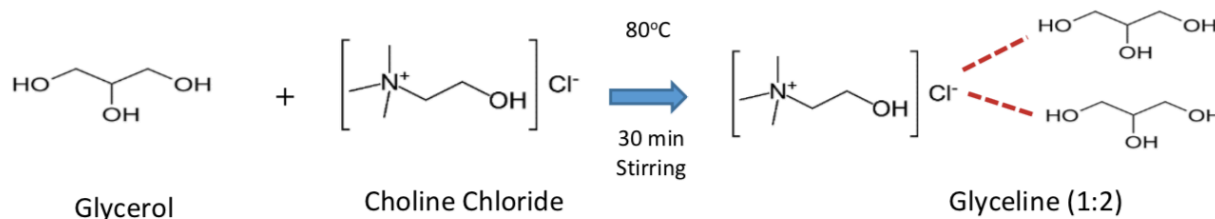
Figure 1. Synthesis of glyceline. Taken from (Orejuela et al., 2017)

Effects of DES solvent in biomass

Different DESs mixtures might have a higher selectivity for certain biomass components, this means that some DESs may dissolve cellulose while others may plastify lignin and extract it from the lignocellulose matrix along with hemicellulose. Solubility test of biopolymers, through the cloud point method (controlled addition) have shown that some DESs are great lignin dissolvers while leaving cellulose fraction intact (W. Zhang, Barone, & Renneckar, 2015)(Orejuela et al., 2017). Moreover, ChCl-oxalic acid DES can be used to achieve 57.9% wheat straw delignification (Lei et al., 2017). Another example of this type of DESs are those prepared with choline chloride and glycerol (Orejuela et al., 2017), lactic acid or glycerine. On the other hand, treating poplar with ChCl-lactic acid at 145 for 6 h, achieved an impressive lignin removal percentage of 78% (Ma et al., 2016).

Micro and Nanocellulose as Materials: Production, Properties and Industrial Uses

Microcellulose is a valuable chemical that has been extensively applied in paper, textile, food and coating industries (O. H. Lin et al., 2016). Its chemical structure is exactly the same as cellulose and nanocellulose, however, the main difference relies on the physical structure.

Microcellulose have micro-size diameter and can have micro or milli-size length as well as it has amorphous and crystalline structures (Reubroycharoen et al., 2018).

Nanocellulose is a nano fiber that can be found in several forms depending of its production method, however, all of its configurations have a diameter between 5-70 nm while its length can be a few nm or several micrometers (Mishra, Sabu, & Tiwari, 2018). There are 3 main types of nanocellulose: nanocrystalline cellulose (NCC), nanofibrillated cellulose (NFC) and bacterial cellulose. NCC is commonly produced by chemical methods like acid or alkali hydrolysis, oxidation or TEMPO oxidation (Mondal, 2017). Acid hydrolysis, which is commonly used (Marcus, 2018)(N. Lin & Dufresne, 2014), degrades the amorphous section of cellulose generating short-rode shape like crystalline molecules with a diameter of 2-20 nm and a length ranging between 100-500 nm (Reubroycharoen et al., 2018). In addition, its crystallinity can be as high as 54-88%. On the other hand, NFC is synthetized by mechanical methods like high-pressure homogenization, ultrafine grinding and ball milling by applying stress and high shear force. This can be accomplished with the use of a ball mill that generates long fibril shapes characterized by a diameter of 1-100 nm and 500 to 2000 nm in length. As the process in not destructive the amorphous region is conserved resulting in a fiber with both the flexible and amorphous regions (Reubroycharoen et al., 2018).

Micro and nanocellulose impressive physical properties make it suitable for several and substantial industrial and medical applications. Due to its high tensile strength (> cast iron) and high stiffness (> Kevlar fiber) they has been used in several polymers such as rubber, cellulose acetate, polyvinyl alcohol and polylactide acid (PLA) as a filler reinforcer of its structure with great results (Jayaramudu et al., 2019). Another important use is in the food and beverage industry were nanocellulose is implemented as a composite in packaging material due to its edibility, nontoxicity, hydrophilic nature, biodegradability. The food packaging industry investigation is mainly focused on improving barrier performance to gases and liquids, ultraviolet rays and in increasing strength stiffness and heat resistance (Kenny, Torre, & Fortunati, 2019) An illustration of barrier properties can be seen in Annex 4 (Adnan et al., 2016). Finally, it is used in the biomedical area as a wound dressing due to its "biocompatibility, substantial water holding capability, superior flexibility, porosity, cell compatible 3D network and excellent durability" (Mishra et al., 2018).

Xylan as a Valuable Material

Xylan biopolymer can be used for several applications, one of them is as food packaging in the formation of bioplastics. Biofilms have been formed solely from xylan or in combination with PVA, nanofibrillated cellulose, chitosan, glycerol etc. All combination aim to improve xylan poor hydrophobicity and film resistance (Naidu et al., 2018). Moreover, xylan hydrogels are used in medical fields like injectable engineering, controlled drug release, biosensors and articular cartilage tissue engineering. They are biocompatible, degradable and promotors of cell adhesion (W. Zhao, Glavas, Odelius, Edlund, & Albertsson, 2014). Other applications include the generation of valued chemicals such as ethanol, furfural, lactic acid and xylitol from monomeric xylose after a hydrolysis process (Naidu et al., 2018).

The aim of this research is to isolate the biopolymers xylan and cellulose from BSG biomass samples to investigate whether the proposed process of using a deep eutectic solvent, an alkali extraction of xylan and bleaching of isolated polymers is a suitable path to obtain microcellulose and xylan biopolymers. Also, ultrasonication is performed on samples to evaluate if smaller structures are achievable. To the best of our knowledge no isolation of biopolymers from BSG biomass has been performed with the proposed pretreatment path.

MATERIALS & METHODS

Materials

BSG was gently donated by the Ecuadorian brewery Cervecería Nacional that has its main production plant in Cumbayá, Ecuador. ChCl (99%) was purchased from HiMedia Laboratories Pvt. Ltd (India). MCC standard was obtained from Sigma-Aldrich. Other reagents such as NaOH, H_2SO_4 were provided by the Laboratorio de Química of Universidad San Francisco de Quito

Brewer's Spent Grains Characterization

Total Moisture Content Determination

Total moisture content was determined by weighting the obtained BSG samples before and after 24 hours of oven drying at 105   according to the ASTM method for Direct Moisture Measurement of Wood and Wood-Based Materials (American Standard Testing Material, 2003). The formula used is:

$$\%MC = \frac{Dry\ Sample\ Weight}{Initial\ Sample\ Weight} \times 100\%$$

Where %MC stands for total moisture content.

Ash Content

The ash content was determined following the NREL modified procedure for "Determination of Ash in Biomass" (Sluiter et al., 2008). Porcelain crucibles were sterilized and dried at 550   for 4 hours and then weighted. 0.5 g of extractive free ground BSG sample were weighted on the crucibles and heated at 550   for 4 hours. The ash content was recorded to use the following formula:

$$\%AC = \frac{Weight_{crucible\ plus\ ash} + Weight_{crucible}}{Initial\ Sample\ Weight} \times 100$$

Where AC is total ash content.

Extractive-free BSG biomass

Extractives free BSG biomass was obtained by following a modified version of ASTM Standard Test Method for Preparation of Extractive-Free Wood (ASTM, 2013). 20 grams of Ground BSG sample were placed in three Soxhlet reflux system with deionized water for a total extraction time of 4 hours. Then, biomass was extracted ethanol 90% for 4 additional hours. Afterwards, the liquors were dried at low pressure in a rotavapor to determine total extractive content.

Lignin Content

Lignin content was determined following the AOAC Official Method 932.01 for "Lignin in Plants Direct Method" (Biomedicas, 2018). Thus, 0.5 g of extractive free ground BSG biomass was digested, under constant stirring, with 15 ml of 72% sulfuric acid for 2 hours. The solution was placed in a reflux system with additional 125 ml of distilled water to each round-bottom flask for 4 hours. Then, the sample was rinsed with water in a filtration system and dried at 105   for 3 h. The equation for lignin content determination is the following:

$$\%LC = \frac{Weight_{crucible\ and\ biomass\ after\ reflux}}{Initial\ Sample\ Weight} \times 100$$

Where LC is total lignin content.

Cellulose Content

      Cellulose content was determined following the methodology proposed by Dominguez et al. (Domínguez-Domínguez, Álvarez-Castillo, Granados-Baeza, & Hernández-Campos, 2012). by digesting 0.5 g of ground BSG biomass sample with 15 ml of 80% acetic acid and 1.5 ml of concentrated nitric acid in a constant reflux system for 20 mins. Samples was washed with water and placed in a previously weighted sterile crucible to oven dry at 60   for 24 h. The dry biomass weight was recorded. Later, the sample was heated at 550   for 6 hours until only ash remained in the crucible and weighted for final calculations:

$$\%CC = \frac{Weight_{crucible\ plus\ biomass\ after\ reflux} - Weight_{crucible\ plus\ ash}}{Initial\ Sample\ Weight} \times 100\%$$

Where CC is total cellulose content.

Protein Content

      Protein was determined by Kjeldahl method according to 981.10 method of the AOAC International (Maehre, Dalheim, Edvinsen, Elvevoll, & Jensen, 2018). The extractive free ground BSG biomass was digested with sulfuric acid (98%) in the presence of a catalyst. After cooling, 50 ml of distilled water was added. The samples were placed in digestion tubes at the distilling unit with additional 50.0 ml of 35% (w/v) NaOH. The distillate collected is titrated with 0.198 N HCl to determine the total nitrogen concentration in biomass:

$$\%N = \frac{V_{HCl} \times C_{HCl} \times P_{eq}}{Samole\ weight\ (mg)} \times 100\%$$

Where, N is the nitrogen content, V_{HCl} is the volume of HCl used for titration, C_{HCl} is the concentration and P_{eq} is it`s equivalent weight. The total protein content is determined by multiplying the nitrogen % by a cereals protein factor (ITW Reagents, 2007):

$$\%Protein = \%N \times 6.25$$

Biomass Pretreatment Methods

Ground BSG biomass was separately pretreated with ChCl/glycerol DES and autohydrolysis (AH) to compare the delignification degree and polymer extraction efficiency between both processes. All experiments were done in triplicate. The two pretreatment methods were performed at two different temperatures, 105 and 125   , for 4 hours, representing a total of four experiments:

Table 1. Experimental design

Experiment label	Pretreatment	Temperature ( )	Time (h)
DES105	DES	105	4
DES125	DES	125	4
AH105	Autohydrolysis	105	4
AH125	Autohydrolysis	125	4

Deep Eutectic Solvent Preparation

A fresh DES mixture was prepared by mixing chlorine chloride and glycerol (1:2 molar ratio) at 80   , in a water bath, until a transparent solution was obtained. The mixture was stored at 4   until use.

Deep Eutectic Solvent Pretreatment

Before pretreatment, samples were grounded and screened with a 40-mesh screen. 4 g of grounded and extractive free biomass was mixed with ChCl/glycerol DES at 1:10 ratio (m/v). Then, it was placed in a Small Quart Benchtop Autoclave Sterilizer at 105 and 125   for 2 hours. Afterwards, the reaction mixture was washed with boiling DI water and ethanol 90% to remove lignin fractions and hemicellulose oligomers/monomers and extracted by the DES. Then, pretreated biomass was dried at 105   to a constant weight.

Autohydrolysis Pretreatment

In autohydrolysis (AH) method, 4 g of grounded and extractive free BSG biomass were mixed with DI water at 1:10 (m/v) ratio. Samples were placed in an Small Quart Benchtop Autoclave Sterilizer again at 105 and 125   for 4 hours. Then, they were washed with DI water and ethanol 90% and dried to a constant weight. Finally, all samples were weighted to calculate lignin extraction yield.

Extraction yield of samples on ChCl/glycerol DES and water are calculated according to equation 5:

$$EY(\%): \frac{m_0 - m_1}{m_0} \times 100\%$$

Where, m_0 is the initial dried sample weight while m_1 the dry sample weight after pretreatment.

BSG Xylan Alkaline Extraction

The pretreated BSG biomass was extracted with sodium hydroxide (1M) at a solution ratio of 1:40 (m/v) for xylan fractionation following Zhang et al. protocol (W. Zhang et al., 2015). The extraction was performed at constant agitation with a stirring magnetic bar for 24 hours and later vacuum filtered to separate the solid residue and the supernatant. The residual biomass, which is identified as cellulose rich fraction, was washed with 100 ml of 1 M sodium hydroxide solution and 100 ml of deionized water. The washing liquors were collected and combined with the supernatant. Resulting cellulose rich fraction was thoroughly washed with deionized water until neutral pH.

Alkaline extract solution from previous step was neutralized with acetic acid. Later, it was mixed with 200 mL of methanol and let to rest overnight to precipitate xylan. Then, the solution was centrifuged to isolate xylan. Then supernatant was put in the rotavapor to reduce its volume to 100 mL and then xylan precipitated again with methanol.

BSG Cellulose and Xylan Bleaching and Drying

Bleaching process has the purpose of extracting residual hemicellulose and lignin from lignocellulose pretreated biomass. The obtained cellulose and xylan fraction samples where bleached with a 5% sodium hypoclorite solution for 24 hours, at room temperature (Kristiansson, 2012) and washed with distilled water until a colorless supernatant was observed. Samples were dried by two different ways: oven-dry and lyophilization; to compare the effect of the different methods of drying in biomass morphology. Lyophilization is freeze drying process were first samples temperature is dropped down to -40   and then pressure is lowered so that water sublimes   (Meg LaTorre-Snyder, 2017). Figure 2 illustrates the sequential processes and experiments performed.

Physical Characterization

FTIR analysis

Infrared spectra of samples were performed using a FTIR spectroscopy (Cary 630 FTIR spectrometer from Agilent Technologies) with a Smart iTR module with Attenuated Total Reflectance (ATR) equipped with Microlab PC software, located in the chemistry labs of USFQ. The chosen wavenumber range was between 4000 and 400 cm^{-1} at a 5 cm^{-1} resolution, which is appropriate to determine the most prominent polysaccharide bonds.

XRD Investigation – Crystallinity Index Determination

X-ray diffraction (XRD) was carried out to investigate the crystalline structure of the samples using an a D8 Advance diffractometer from Bruker Corporation with K-beta radiation from DEMEX Metallurgy Institute of Escuela Politécnica Nacional del Ecuador (EPN). The examination was performed with a locked couple 2θ scan profile at an angle range from 3 to 80 °. The sample was crushed to powder and placed in a special instrument sample holder. The formula

described by Segal equation (Segal, Creely, Martin, & Conrad, 1959) was used to calculate crystallinity index (CI) of the experiment samples and control:

$$CI = 100 \times \frac{I_{020} - I_{am}}{I_{020}}$$

Where I_{020} is the peak intensity at a plane (020) (arbitrary units) in the XRD profile and I_{am} is the minimum intensity corresponding to amorphous sections at $2\theta = 18°$.

Differential Scanning Calorimetry (DSC)

Determination of thermal points for samples were determined by Differential Scanning Calorimetry Q2000 DSC from TA instruments, located at EPN. The analysis was performed by heating samples at a scanning speed of 10 min^{-1} from 25 to 350 .

TGA Analysis

Thermal degradation properties of the materials in a range from 25 to 600 were analyzed with a TGA-50 detector from CIAP polymer institute of Escuela Politécnica Nacional del Ecuador. 10- 20 mg were placed in the sample holder and heated at a rate of 10 /min from 25 to 600 . To simplify visualization, the thermal graph was expressed in terms of (%) weight lost vs. temperature.

Scanning Electron Microscopy (SEM)

An IT500 Intouchscope SEM purchased from JEOL USA, located at Mechanical Engineering Department Materials Laboratory of USFQ, was used to examine the micro or nano fibrillation of the samples at 4 different pretreatment conditions. Samples surface was scouted to find fibrillated or fractionated sections for evidence of micro or nanocellulose presence.

```
                    ┌─────────────────────┐
                    │    Grounded BSG     │
                    └─────────────────────┘
                               │  DI water (4h)
                               │  Ethanol 72% (4h)
                    ┌─────────────────────┐
                    │  Extractives-free BSG │
                    └─────────────────────┘
   ChCl/glycerol (1:2 molar                    DI water
         molar)
   ┌──────────────────────┐      ┌──────────────────────────┐
   │  ChCl/gly pretreatment │      │ Autohydrolysis pretreatment │
   │ (1:10 m/v) (105, 125 ℃, 4h) │ │ (1:10 m/v) (105, 125 ℃, 4h) │
   └──────────────────────┘      └──────────────────────────┘
                          Vacuum filtration
                    ┌─────────────────────┐
                    │   NaOH Extraction   │
                    │ NaOH(1M) (1:40 m/v) (24 h) │
                    └─────────────────────┘
       ┌──────────────────┐       ┌──────────────────┐
       │ Cellulose filtrate │       │   Hemicellulose   │
       └──────────────────┘       │    Supernatant    │
                                   └──────────────────┘
                                       Neutralize with acetic acid
                                       Methanol 99%
                                   ┌──────────┐
                                   │   Xylan  │
                                   └──────────┘
              NaOCl 5% solution
                    ┌──────────────────────────┐
                    │        Bleaching         │
                    │ NaOCl (5%):biomass (10:1 v/m) │
                    └──────────────────────────┘
       ┌──────────────────┐       ┌──────────────────┐
       │   Oven-drying    │       │  Lyophilization  │
       └──────────────────┘       └──────────────────┘
```

Figure 2. Scheme of the process of isolation of cellulose and xylan from BSG biomass using ChCl/glycerol deep eutectic solvent

RESULTS AND DISCUSSIONS

BSG Characterization Results

Native ground BSG biomss was characterized in triplicate, table 2 summarizes the results obtained. The moisture and ash content found were 75.29 $\pm$0.10 and 4.00 $\pm$0.01 respectively, which are in accordance with the values in literature. Alexander et al. (2015) found that the BSG from a brewery in Rio de Janeiro had 82.60 $\pm$0.10 moisture and 3.8 $\pm$0.00 ash content. On the other hand, Santos et al. evaluated the same parameters for barley based BSG and established that moisture content was between 76.80 and 78.90% while ash content ranged from 3.40 and 4.00% (Z. Li, Yan, Shen, & Ding, 2012). Extractives from biomass account for 7.25 $\pm$1.15% as it can be appreciated in table 2, and is comparable to the value of 10.73 $\pm$0.32% determined by Meneses et al. (Meneses, Martins, Teixeira, & Mussatto, 2013). This classification may include waxes, alkaloids, pectins, mucilages, gums, resins, terpenes, saponoids and tall oil in BSG. Moreover, lignin, cellulose and protein content were found to be 15.15 $\pm$2.48, 22.58$\pm$1.63 and 33.95$\pm$0.60, respectively. These results agree with lignin (19.27$\pm$0.34), cellulose (ranging from 16.78 and 21.73. $\pm$1.36) and protein reported values (24.69) (Meneses et al., 2013)(Mussatto & Roberto, 2006). Protein values are slightly higher than the reference showing that the biomass used in this study was rich in protein. Hemicellulose has been calculated by difference.

Table 2. Compositional Analysis of ground BSG native biomass

Compositional Analysis	Percentage (%)	Method
Moisture content	75.30 $\pm$0.10	(American Standard Testing Material, 2003)
Ash Content	4.00 $\pm$0.01	(Sluiter et al., 2008)
Extractives	7.25$\pm$1.15	(ASTM, 2013)
Lignin	15.15$\pm$2.48	AOAC 932.01
Cellulose	22.58$\pm$1.63	(Domínguez-Domínguez et al., 2012)
Protein	33.95$\pm$0.60	AOAC 981.10
Hemicellulose	21.07	Calculated by difference

Effect of Pretreatments on Extraction

     Solvents have the ability to dissolve specific biomass components. As mentioned before, ChCl/glycerol DES pretreatment softens and cleave lignin-carbohydrate bonds and selectively extracts lignin along with some hemicellulose (Orejuela et al., 2017) while in autohydrolysis hemicelluloses are hydrolyzed as oligosaccharides, sugars and aldehydes dissolving in higher rates in water (Aguilar-Reynosa et al., 2017). Precisely, acetyl groups of hemicellulose are cleaved and form acetic and phenolic acids forming an low pH medium that facilitate hydrolysis of biomass components cellulose, hemicellulose and lignin (X. Zhao, Cheng, & Liu, 2009). For this reason, more polymeric structures would dissolve. Moreover, A percentage of cellulose is converted to glucose and would be present in the liquor so that the cellulose yield would be lower in the case of autohydrolysis pretreatment than in the DES pretreatment. Biomass fractionation rates under the 4 experiment conditions are shown in figure 3.
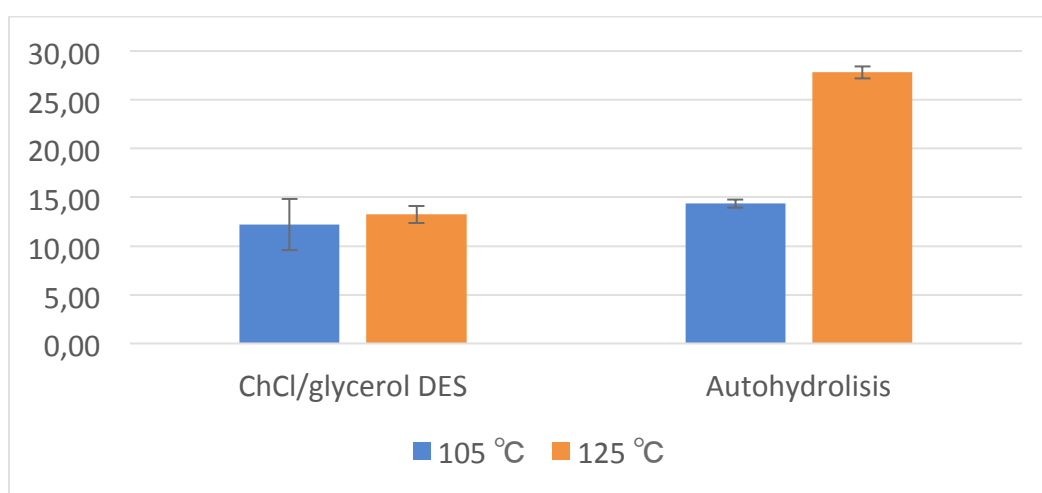
Figure 3. Extraction rate of BSG on ChCl/glycerol pretreatment and autohydrolysis

     All experiments were done for a period of 4 hours. For BSG pretreatment with ChCl/glycerol DES, fractionation increased from 12.20 % to 13.24% as the experiment temperature was set from 105 to 125   meaning that the temperature range studied does not influence greatly in solvent extraction capacity. On the other hand, fractionation of biomass in water did doubled its value going from 13.24% to 27.82 %   among the two experiment conditions, which is in agreement with increasing extraction rates with temperature as reported by Zhang et al. (2015). However, the total lignin content represents 15.15 $\pm$2.48 % as shown in

table 2, so the high biomass loss in autohydrolysis has to account for polysaccharide depolymerization while the consistent DES extraction values around 14.00% might be related to lignin selective extraction. For the purposes of this study it is more important to preserve polysaccharides for further isolation.

Biopolymer Extraction Efficiency

Alkaline extraction and bleaching were performed on pretreated biomass to obtain a better-quality product, with low hemicellulose and lignin content. The biopolymers extraction rates from initial biomass, and percentage of recovery are shown in Table 3.

Table 3. Biopolymers Extraction Rates and Recovery from initial quantities

Experiment Label	Cellulose Extraction (%)	Cellulose Recovery (%)	Xylan Extraction (%)	Xylan Recovery from Hemicellulose (%)
DES105	18.56	82.22	10.77	74.55
DES125	19.40	85.93	11.12	52.79
AH105	13.63	60.35	10.14	48.13
AH125	10.75	47.63	6.11	29.01
Initial Value	22.58	100.00	21.07	100.00

It can be observed that cellulose extraction slightly increased in DES pretreatment with temperature raise from 105 to 125 ^{o}C. This small change demonstrates that both conditions have similar extraction capacities. On the other hand, autohydrolysis (AH) have lower cellulose extraction rates than DES pretreatment. Moreover, AH105 cellulose extraction is 3% lower than AH125. This can be explained by referring back to the analysis that stated that more polysaccharides are been lost in the AH pretreatment and that at higher temperatures autohydrolysis is even more radical in polymers extraction. Xylan isolation from BSG has not been reported before, however, analysis of acid hydrolysates have a percentage composition of 37 to 48 % xylan (Mussatto & Roberto, 2006). The xylan extraction rate ranges from 6.11 to 10.77 % which is about half of total hemicellulose content (21.75%). This is in agreement with literature that report that xylan in grasses can be half of total hemicellulose content. On the other hand, the same tendency of this hemicellulose lost is observed in autohydrolysis pretreatment in comparison to the use of DES solvents.

FTIR Spectra Analysis

Figure 4 represent the FTIR spectra analysis and allows to monitor functional group differences among the 4 different cellulose samples and compare it to MCC cellulose standard (DES105, DES125, AH105, AH125).
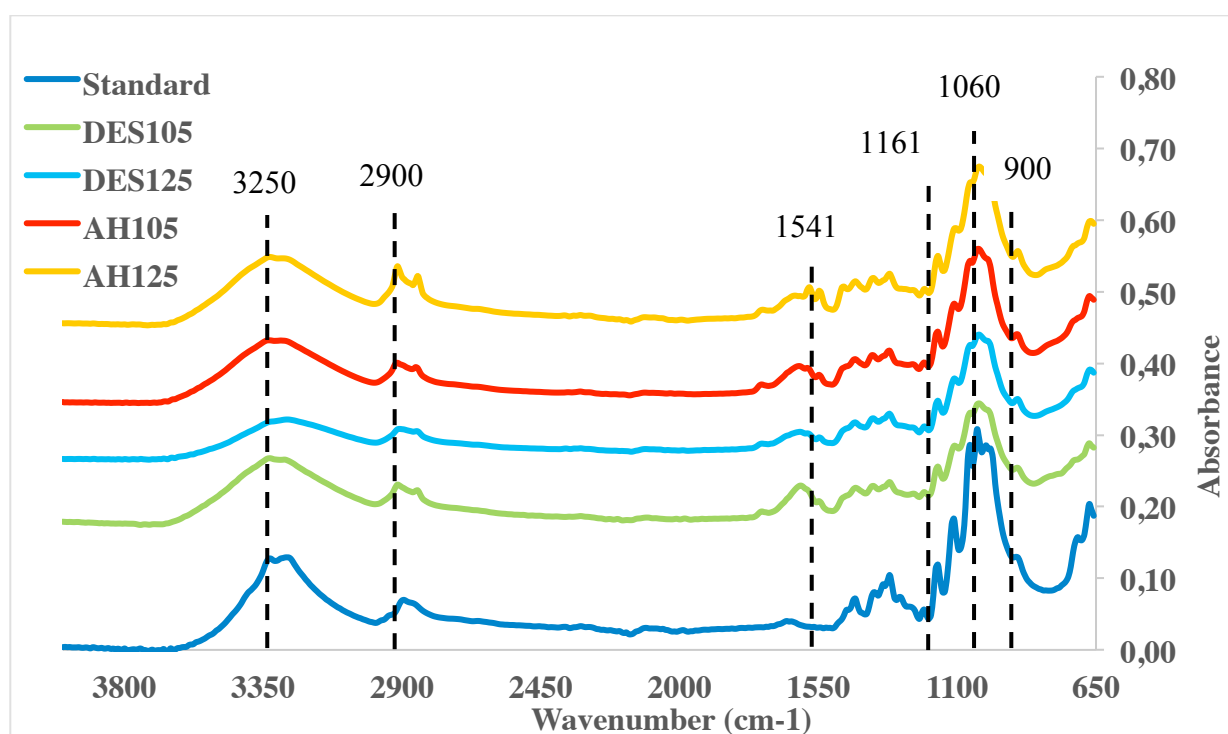
Figure 5. Cellulose FTIR spectra of BSG biomass samples

The strong peak at 1060 cm^{-1} and 1010 cm^{-1} indicate the presence of C-O, C-O-C and C-C stretching of typical cellulose repeating unit, cellobiose (see Annex 5). Kondo et al. (2016) report these peaks at 1060 and 1030 cm^{-1} for bacterial nanocellulose. Moreover, the band at 1160 and 900 cm^{-1} has been assigned at the $\beta - (1,4)$ glucosidic linkage of cellulose and agrees greatly with typical reported values 1161 and 900 cm^{-1} (Kondo et al., 2016) (Lee, Sundaram, Zhu, Zhao, & Mani, 2018). The frequency from 1541 cm^{-1} represent C=C in lignin aromatic rings which contrast with the absence of the same peaks for MCC standard. Aquino et al. report this peak for alkali and bleached cellulose at 1526 cm^{-1} (Aquino, Signini, Bukzem, Ascheri, & Santos, 2015). C=O double bound from carbonyl groups, probably formed after hydrogen

bonding cleavage of cellobiose hydroxyl groups, is located at 1630 cm^{-1}, which agrees with the band 1650 cm^{-1} found by Kondo et al. (2016).

Furthermore, the peak at 1719 cm^{-1}, reported by Aquino et al. at 1734 cm^{-1}, non-existent in the standard, represent the acetyl and uronic ester groups of hemicellulose or the ester linkage of carboxylic groups of ferulic and p-coumeric acids of lignin (Aquino et al., 2015). This demonstrates the presence of residual hemicellulose and lignin in small quantities due to weak peaks. Finally, the peak at 3250 cm^{-1} and the shouldering at 3320 cm^{-1} indicates the presence of O-H stretching while the peak at 2980 cm^{-1} accounts for the asymmetric stretching vibration of C-H bonds (Wang, Yao, Zhou, & Zhang, 2017). Wang et al. reported O-H and C-H peaks at 3340 and 2900 cm^{-1} respectively for cotton cloth nanocrystals. The shift of samples peak from 2900 to 2980 cm^{-1} can be attributed to formation of new hydrogen bonds after delignification and extraction of hemicellulose (Pan, Zhao, et al., 2017). After, the analysis all samples show strong evidence of been cellulose.

Xylan physicochemical and conformational structure is analyzed in figure 5. Samples are compared and contrasted with MCC standard as the two molecules share various common peaks and functional groups.
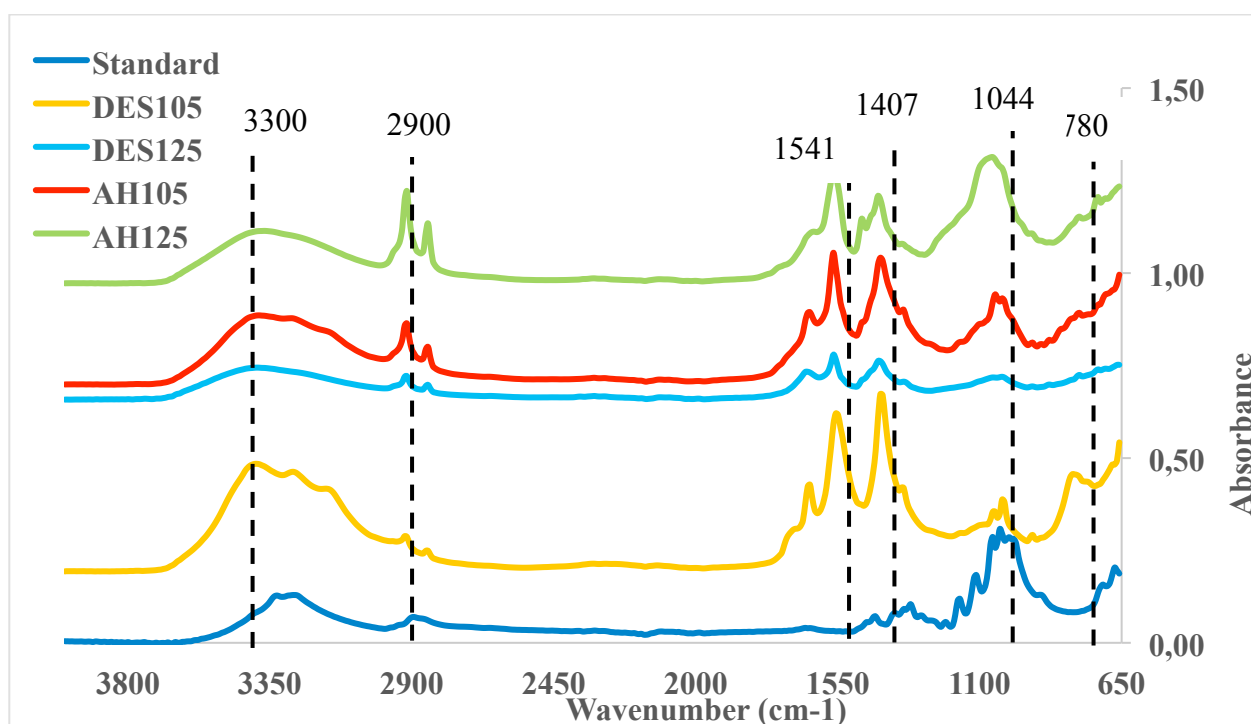

Figure 6. Xylan FTIR spectra of BSG biomass samples

The signal from $750\ cm^{-1}$ corresponds to typical $\beta - (1,4)$ glucosidic linkage xylan backbone which Palaniappan el al. define the in region of 835 to $840\ cm^{-1}$ (Palaniappan, Yuvaraj, Sonaimuthu, & Antony, 2017). The peak at $1044\ cm^{-1}$ is shared with MCC standard and denotes the C-OH and C-C stretching bonds that both xylan and cellulose share. On the other hand, the two most prominent signals that form a "M", not present in MCC standard, are characteristic of the xylan structure. The absorbance at $1407\ cm^{-1}$ correspond to CH_2 stretching bonds, which are common in hemicellulose, and the one at $1541\ cm^{-1}$ is attributed to uronic acid carbonyl groups. Sun et al. report these peaks at 1415 and $1592\ cm^{-1}$ respectively for sweet sorghum stem xylan extracted with alkali and organic treatment (2013). Uronic acid peak is typical for arabinoxylan (S. L. Sun et al., 2013) which means that samples extracted in this study probably contain a mixture of arabino and homoxylan. The uronic acid signal extends to $1720\ cm^{-1}$ and can also have lignin groups contribution from residues as mentioned above for cellulose (Aquino et al., 2015). Finally, peak at 2900 and $3300\ cm^{-1}$ relate to C-H and OH stretch (Savitha Prashanth & Muralikrishna, 2014) and are shared with cellulose. In this sense, the structures found are strong evidence that all hemicellulose samples are xylan.

Crystalline Structure Analyses

The XRD study was performed on MCC standard, DES105, DES125, AH105 and AH125 to identify the type of cellulose obtained and its overall crystallinity.

The samples showed a main peak at (020) diffraction plane, positioned at $2\theta = 22.5$ °, which is characteristic of type I cellulose (Bohn, 2017). These diffractograms are typical of semi-crystalline structures with wide peaks that account for crystallinity of semi-crystalline materials and humps for amorphous sections (O. H. Lin et al., 2016) as it can be seen in Figure 7. The degree of sample crystalline structure is shown in table 4.

Table 4. Crystallinity of samples

Sample	I_{020}	I_{am}	$C_I^{XRD}(\%)$
MCC Standard	85.00	3.00	96
DES105	32.00	19.00	41
DES125	11.00	7.00	36
AH105	22.00	12.00	45
AH125	22.00	12.00	45

Crystalline peaks obtained for all samples, ranging from 0.36 to 0.45, are consistent to values of 38.33% and 45.25% of cellulose extracted from cotton cloth and degreasing cotton respectively (Wang et al., 2017) or to 48.80 % of ultrasonicated pineapple leaf fiber nanocellulose (Mahardika, Arief, Kasim, Abral, & Asrofi, 2018).

DES105 and DES125 samples have lower crystallinity than AH105 and AH125. As mentioned above, since DES pretreatment isolated cellulose more efficiently it might also have destructively broken hydrogen bonding in cellulose fibrils (in lignin separation process) damaging its crystalline structure (Mahardika et al., 2018). Moreover, samples DES125 has lower crystallinity than DES105, which is probably due to cellulose crystalline areas deconstruction due to higher pretreatment temperatures. In this sense, results allow to say that MCC standard can be considered crystalline, DES105, AH105 and AH125 semi-crystalline/amorphous and DES125 amorphous (Bohn, 2017). These results are lower than usual nanocellulose crystallinity (55%)
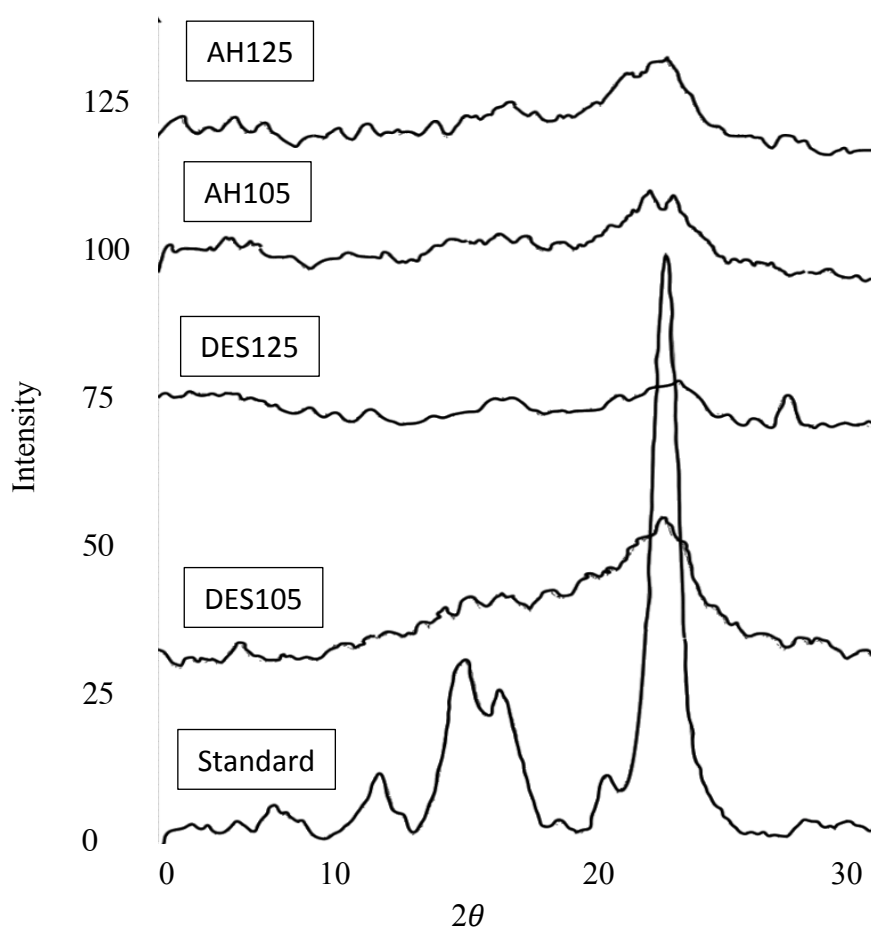
Figure 7. XRD Spectra of DES and Autohydrolysis pretreated samples

produced after acid hydrolysis attack, that is known to cleave glucosidic bonds and release the individual crystallites (Wang et al., 2017). Finally crystallinity might also have been affected by alkali pealing that removed hemicellulose and some amorphous cellulose causing a rearrangement of crystalline sections lowering crystallinity (Pan, Zhao, et al., 2017). Higher values of crystallinity confers DES105, AH105 and AH125 samples better mechanical strength and make them suitable for reinforcing materials (Wang et al., 2017). On the other hand, amorphous cellulose is appropriate for functional group modifications to develop tailored materials for various remarkable applications (Ciolacu, Ciolacu, & Popa, 2010).

DSC Analysis

Thermal properties of micro-cellulose like decomposition temperatures and heat adsorption are studied with the Differential Scanning Calorimeter analysis (DSC). Results of these experiments are shown in figure 8.
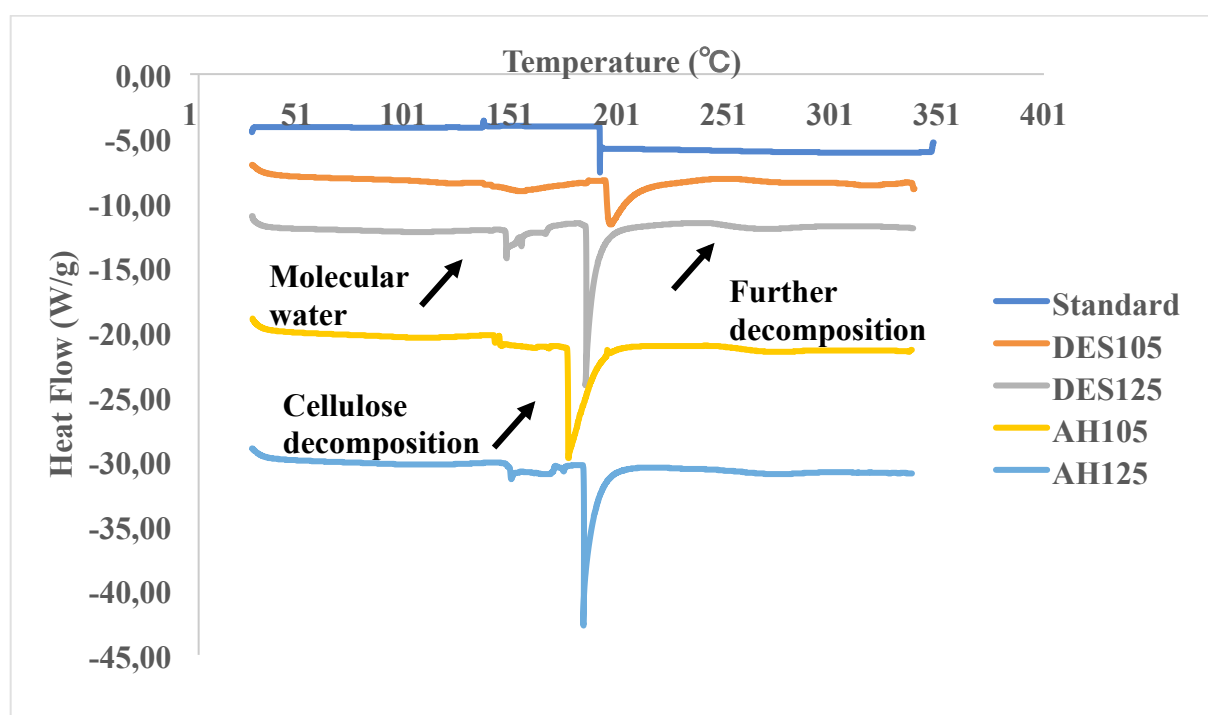
Figure 8. Cellulose DSC analysis

As (O. H. Lin et al., 2016) noted, the endotherm curves for DES105, DES 125, AH105 and AH125 from 30 to 110 , are due to water evaporation from samples. In contrast, MCC standard apparently has no moisture since no heat is absorbed at this region.

Moreover, BSG cellulose samples show a peak around 150 , not present in the standard, that can be attributed to water evaporation interreacting at a molecular level due to samples hygroscopic nature (Kian, Jawaid, Ariffin, & Karim, 2018). Kian research group report the same endothermic peaks between 130 and 160   for samples with different degrees of sulfonation after roselle MCC acid hydrolysis to produce roselle NCC. DES125 and AH125 peaks are larger at this section of the graph, which means that they are more hygroscopic than the rest of the samples since they absorb more energy to evaporate residual water. The reason might be because the experiments conducted at 125   had a larger accommodation of hydrogen bonding due to further cellular wall fractionation (Mahardika et al., 2018) that prompted an increase of interaction with molecular water. Drying temperatures are tabulated in table 5.

Moreover, cellulose is believed to undergo decomposition as polymer chains melt and degrade (Szymańska-Chargot, Chylińska, Pieczywek, & Zdunek, 2019). Large and broad sample peaks for all samples between 180 and 195   are attributed to decomposition of samples due to the high energy absorption at this point.

Table 5. DSC relevant temperatures

| Sample	Molecular water drying ( )	Decomposition Temp. ( )
MCC Standard	-	194.44
DES105	158.03	198.25
DES125	149.20	185.50
AH105	146.21	178.18
AH125	151.56	185.27

Thermal properties of samples are comparable to Kian et al. results that report decomposition points from 202.38 to 212.00 respectively for roselle NCC (Kian et al., 2018).

On the other hand, the larger the peak the more amorphous material content the samples have. All of them, specially DES125 samples have a considerable larger melting peaks than MCC standard which related to the presence amorphous cellulose, lignin and hemicellulose Wang et al. (Wang et al., 2017) demonstrated that purified cotton CNC obtained had shorter

peaks than their corresponding cellulose samples and raw materials and attributed the difference to amorphous components. DES125 has the largest peak, which means it has more residues than the rest of the samples corroborating the low crystallinity obtained. The second largest peak of AH125 might mean that high temperatures in both pre-treatments reduced presence of crystallites. Finally, there are other small endothermic curves for all samples around 250   that represent further cellulose decomposition.
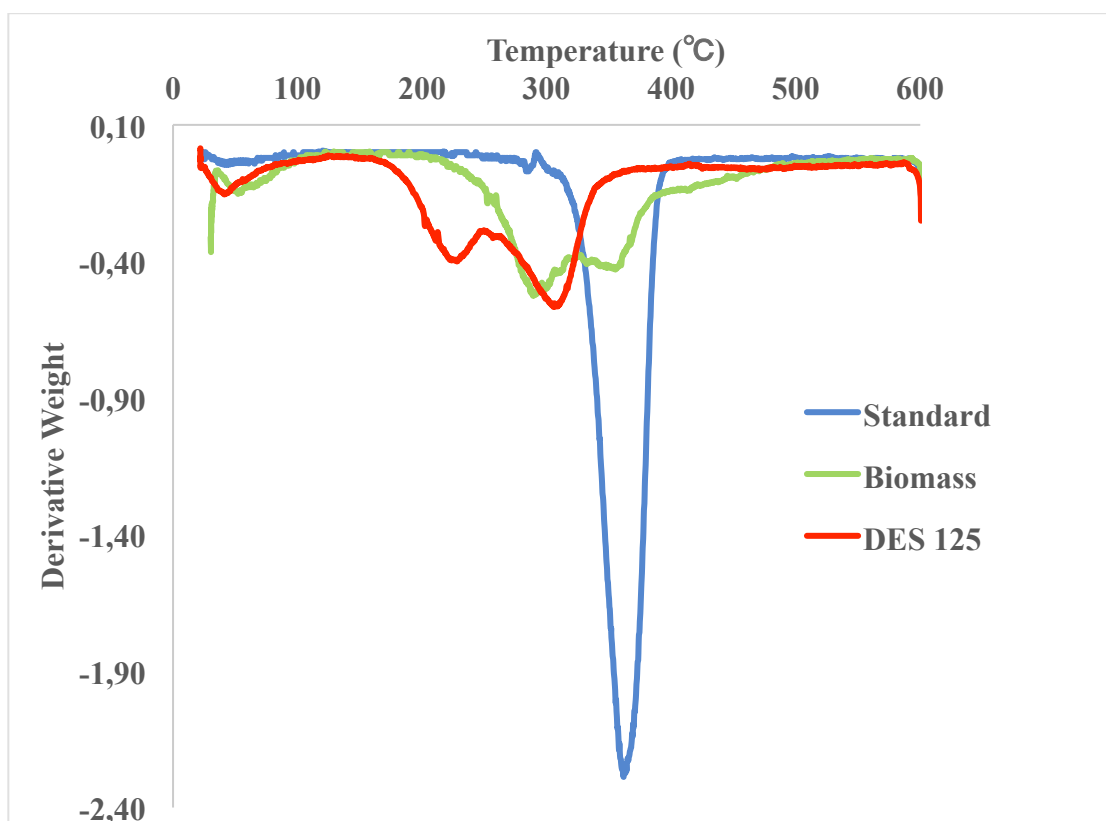
TGA Analysis

At the present section TGA of raw BSG biomass, DES125 and MCC standard were performed to analyze sample weight loss as temperature increased. Representative TGA curves generated at a heating rate of 10   /min are shown in figure 9 while the derivative curves that allow to identify main degradation points can be seen in figure 10.
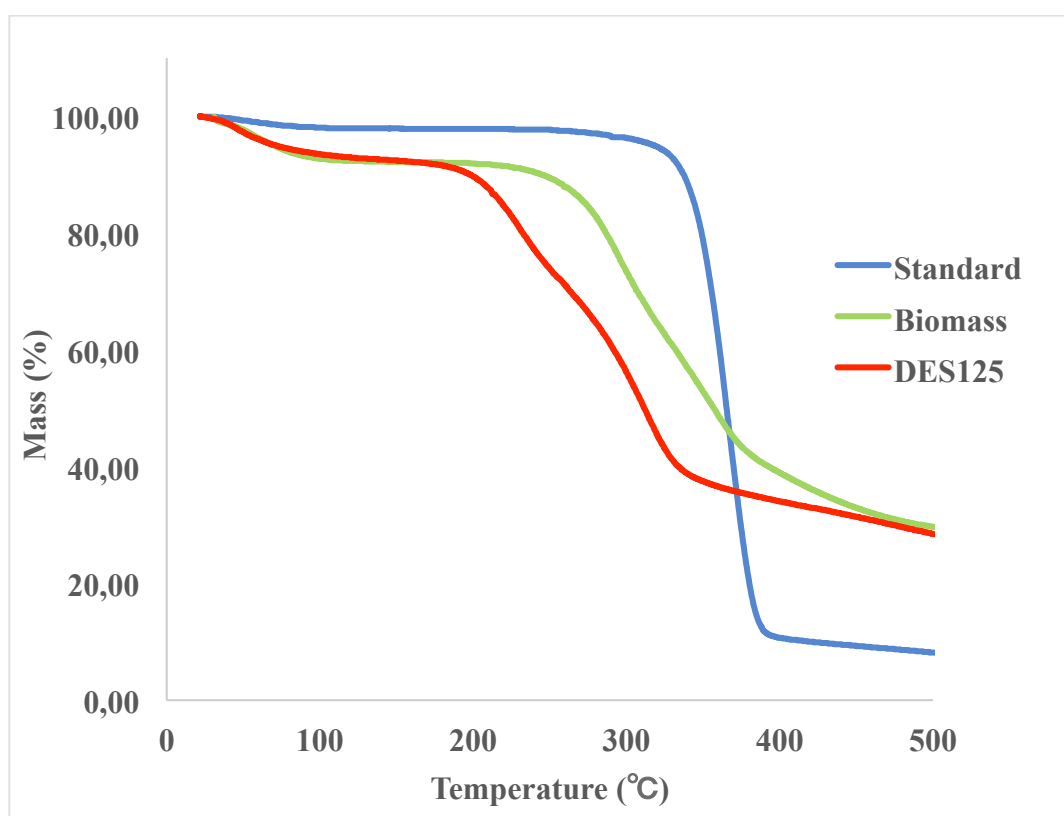
Figure 9. Cellulose TGA curves

Samples initial mass loss from 50 to 100   could be attributed to water evaporation, denoting their hygroscopic nature and corroborating the DSC results. Moisture content of

samples are shown in table 6. T (on) represents the temperature where degradation starts while T(max) stands for the temperature of maximum mass loss. Samples main thermal degradation happen in the range of 175 to 400 . Generally, lignin early degrades from 200 to 700 , hemicellulose from 220 to 300 and cellulose from 250 to 400 (Aquino et al., 2015). In DES125 sample, degradation starts at an early T (on) of 158.00 mainly because residual hemicellulose and lignin promotes degradation (Mahardika et al., 2018).

Figure 10. Cellulose derivative TGA curves

Table 6. TGA and derivative TGA analysis results

| Sample	Moisture Content	T (on) From TGA	T (max) From DTGA	Mass loss (%)
Biomass	7.33	201.70	294.70	71.18
DES 125	7.42	158.00	308.80	71.25
MCC standard	1.98	245.00	363.10	91.80

The mentioned fact can be appreciated in DTGA figure 10. The fist peak of DES125, after T(on), is due to rapid decomposition of hemicellulose that has already been hydrolyzed and weakened in the pretreatment. Right after, a second peak, closer to MCC standard T(max) = 363.10   and corresponding to T(max)=308   is observed. This is related to cellulose degradation related to lignin and hemicellulose decomposition that directly promotes glucosidic bonds cleavage in the process (Feng et al., 2018).

On the other hand, biomass degradation started at a higher temperature T(on) = 201.70   . This probably happened because hemicellulose and lignin polymers were not hydrolyzed by pretreatment and endured better the heat effect. However, biomass T(max) occurs at 294.70 which is considerably lower than DES125 and MCC standard because mass loss higher r related to hemicelluloses and lignin, which combined represent over 30% sample. The second peak on the right of biomass T(max) is related to cellulose degradation catalyzed by the destruction of the other two residual polymers as mentioned before. Moreover, MCC standard T (on) = 245.00 and T(max)=363.10   are higher due to cellulose purity. Feng´s group found T(max) for sugarcane bagasse, bleached cellulose and nanocellulose of 351.30, 353.50 and 352.00 respectively (Feng et al., 2018). These values show that sugarcane bagasse is a more resistant biomass than BSG probably since the second one went through brewing process. On the other hand, DES125 T(max) is close to reference values.

After 400   a slow thermal degradation profile is obtained. Most polysaccharides have depolymerized and reduced to char (Mahardika et al., 2018). However, biomass and DES 125 residual weight is due to remaining slow decomposing lignin (Feng et al., 2018).

Effect of Pretreatments on Morphology

Morphological structures of oven dried MCC standard, DES105, DES125, AH105 and AH125 samples were observed with SEM. The image results are shown next:
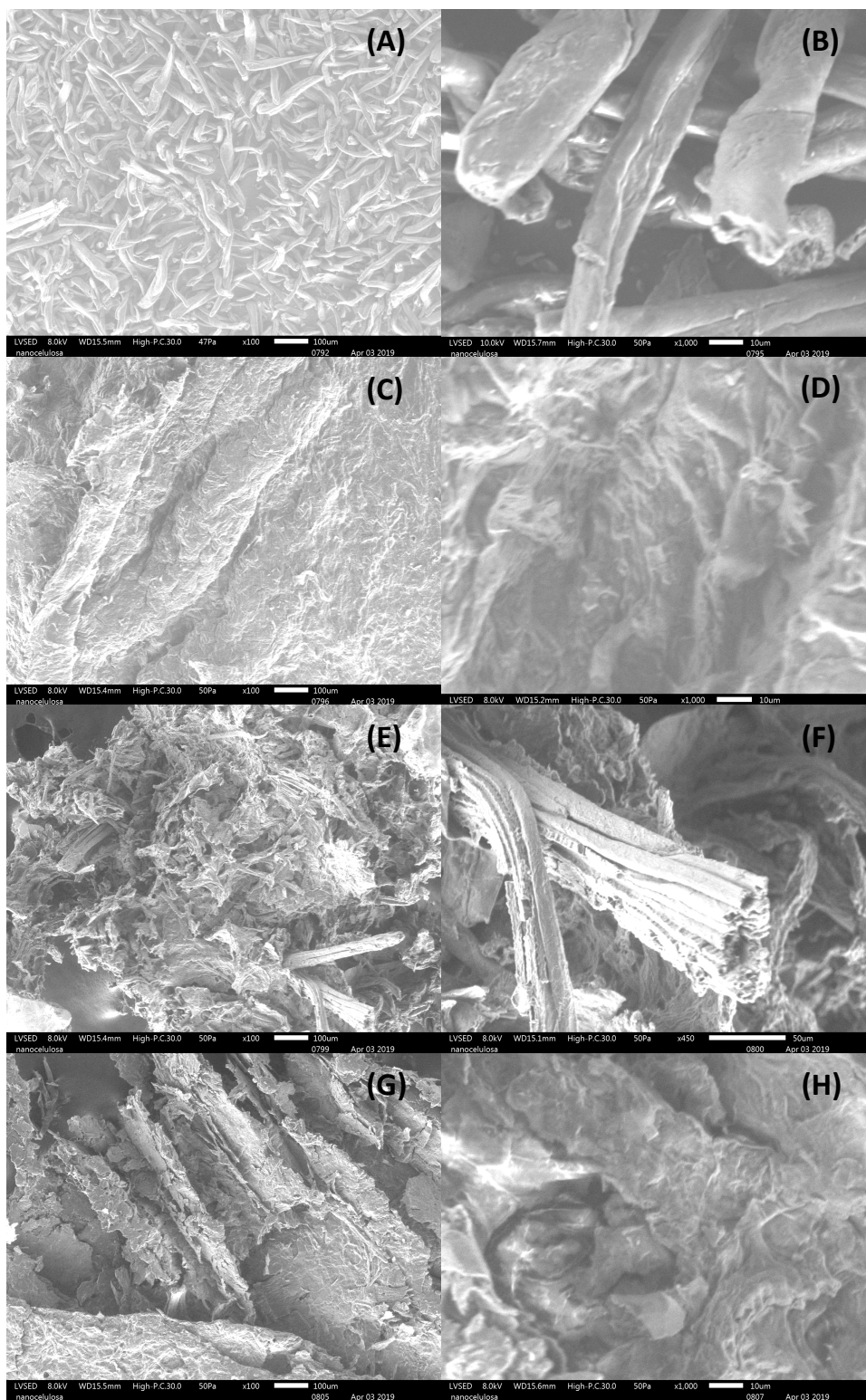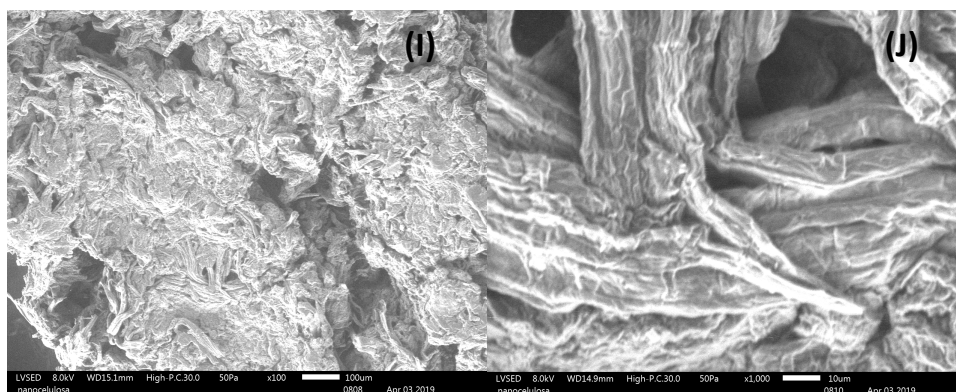
Figure 11: Morphological images of oven dried samples A) MCC standard at 100 *um* scale and at B) 10 *um* scale, C) DES105 at 100 *um* scale and at D) 10 *um* scale, E) DES125 at 100 *um* scale and at F) 50 *um* scale, G) AH105 at 100 *um* scale and at H) 10 *um* scale, I) AH125 at 100 *um* scale and at J) 10 *um* scale.

As it can be seen in figure 11 MCC standard show individual micro size fibrils while the rest of the samples show agglomerations of fibrils, however, not completely separated. The two most probable reasons for this to happen is that lignin and hemicellulose were not completely removed or the fibers were aggregated during drying (O. H. Lin et al., 2016). As an example, Lin et al. team obtains completely defibrillated MCC fibers from empty fruit bunches and sugarcane bagasse after 3 repeating alkali treatments, however, Mandal et al. show that a mass of microfibrils are obtained after single alkali and delignification pretreatment of sugarcane bagasse (2011) very similar to images in figure 11 (See Annex 6). In DES125, a large microfibril is preserved, revealing cellulose unidirectional fibrillated morphological nature and providing evidence of obtaining microfibrils among the cellulose.

DES105 and AH105 samples did not showed evident defibrillation, however, its surface indicated multiple layers stacked due to extraction of cellular wall components (Pan, Gan, Mei, & Liang, 2017). This can also be an effect of alkaline pretreatment that tends to cause the fiber to swell and delaminate (Lee et al., 2018).

Moreover, DES125 and AH125 show signs of fibrillated sections, however, agglomerated fibrils were observed. In any case, the observation of fibrils on DES125 and AH125 samples might be due because structures were well preserved by chance during drying

since they usually tend to stick together (Lee et al., 2018). For these reasons, morphology was investigated with a second drying method.

Morphological structures of MCC standard and lyophilized samples are observed in figure 12.
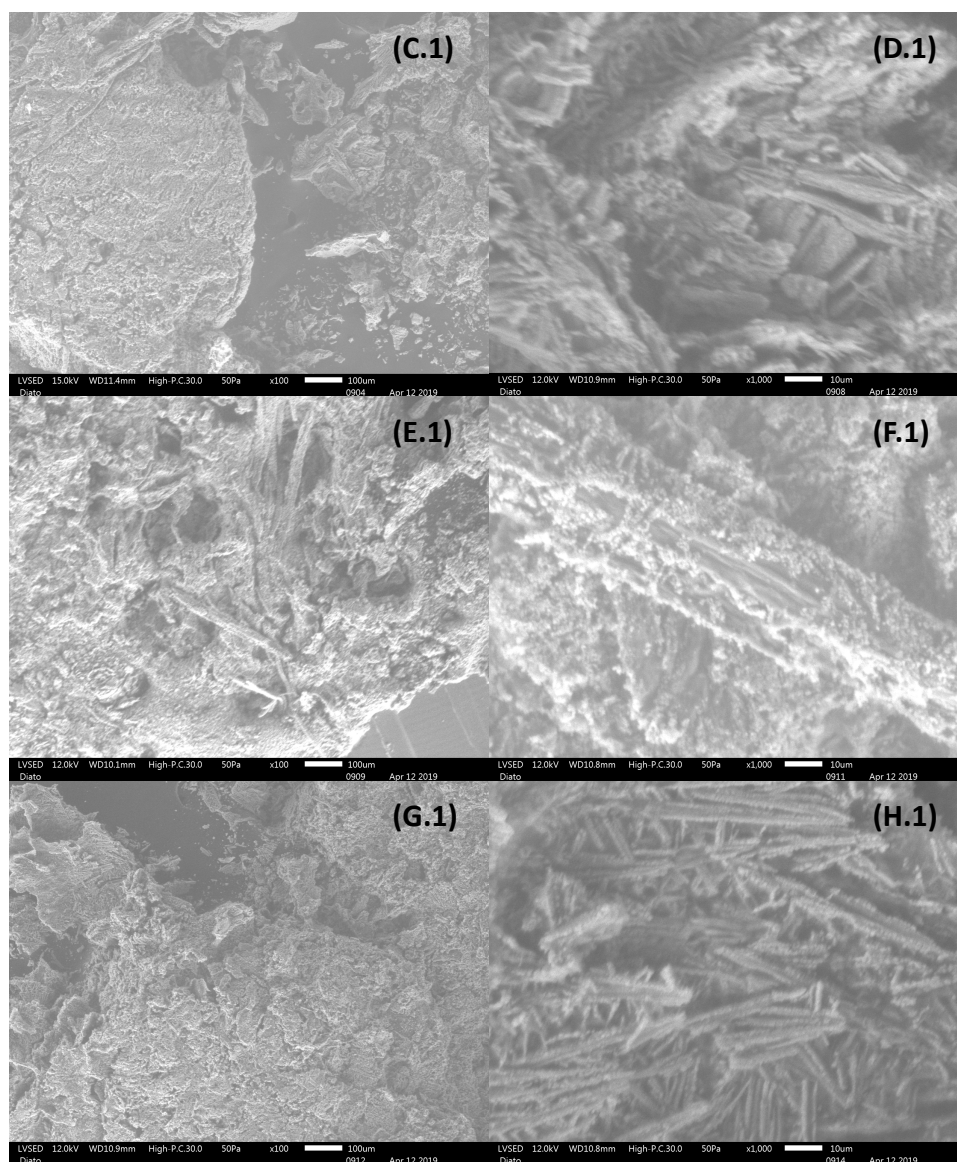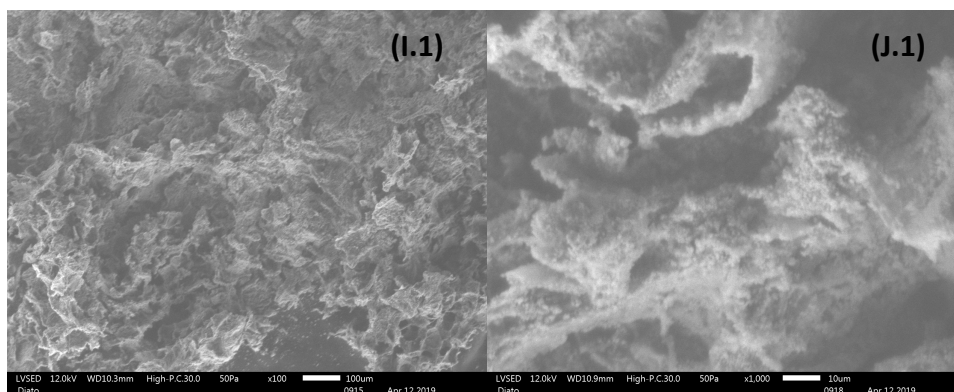
Figure 12: Morphological images of lyophilized samples C.1) DES105 at 100 um scale and at D.1) 10 um scale, E.1) DES125 at 100 um scale and at F.1) 10 um scale, G.1) AH105 at 100 um scale and at H.1) 10 um scale, I.1) AH125 at 100 um scale and at J.1) 10 um scale.

In the case of lyophilization drying, microfibrils seem to have been preserved better except of AH125 sample were the aggressive drying method caused micro explosions or it was laminated because of alkali extraction as mentioned before. This shows that it is not only DES125 and AH125 samples that had fibrils, but all samples show them in specific sections. Samples DES105, DES125 and AH105 visible fibril size diameter seems to range from 1 nm to 100 um, similarly to Aquino et al. (Aquino et al., 2015) obtained carboxymethylated brewer´s spent grain cellulose, after alkali and bleaching, with a fibrils diameter from 5 um to 30 um. However, better image resolution and a higher zoom is necessary to analyze better and more precisely diameter and surface characteristics.

CONCLUSIONS AND RECOMMENDATIONS

ChCl/glycerol DES pretreatment is better for biomass fractionation and polysaccharide isolation since it mainly plasticizes lignin and separates part of it from biomass but does not hydrolyze valuable polymers into oligomers or monomers that are later not recoverable like fibers. It is recommended to consider autohydrolysis as a more appropriate process for ethanol production were at higher temperatures lignin is degraded and monomeric sugars release for fermentation.

Furthermore, FTIR analysis allows to conclude that ChCl/glycerol DES and autohydrolysis with alkali pretreatment and bleaching are efficient methods to obtain cellulosic and xylan

(arabinoxylan and homoxylan) fractions. Also, residual lignin and hemicellulose are present in small quantities and affect the intensity of peaks

XRD analyses corroborates the cellulose isolation and identifies it as cellulose type I. On the other hand, amorphous material residues undermine crystallinity of samples, however, DES105, AH105 and AH125 semi-crystallinity confers them enough mechanical strength for material biocomposites where this property is necessary. On the other hand, they are appropriate for cellulose functionalization applications.

DSC and TGA close examinations allow to conclude that samples have typical cellulose degradation temperature and that DES125 has a high temperature of maximum degradation (308.80   ) which make it suitable for material that need to be moderately heat resistant. Moreover, study shows that thermal properties can be improved by removal of amorphous sections like amorphous cellulose, hemicellulose and lignin to reach MCC standard and nanocellulose properties. In this sense, repetitive alkaline extraction and bleaching are recommended in order to obtain pure cellulose followed by acid hydrolysis or ultrasonication to reduce cellulose size and liberate individual microcrystals.

Finally, in SEM study was observed that the continuous processes performed produced sections of agglomerated, sticked together fibrils, or delaminated layers while in other sections microcellulose was identified revealing fibrillated cellulose nature. Therefore, the continuous pretreatment can partially produce microcellulose. Cellulose morphology should be better preserved through different enhanced sample preparation methods in order to determine is the method does actually generate fibrils.

FUTURE WORK

In future work, methods to obtain pure cellulose and xylan will be investigated, as well as optimization of extraction conditions using other deep eutectic solvents such as choline chloride: urea, choline chloride:lactic acid or choline chloride:oxalic acid. Furthermore, nanofibrillated or nanocrystalline cellulose are going to be obtained via different approaches to produce materials that can be used to make nanocomposites with high resistance and thermally stable. Xylan biopolymer should be characterized and attempts to make biofilms/bioplastics for food industry would be investigated. Moreover, lignin fraction obtained after DES and alkali pretreatment will be isolated from supernatants to study their molecular weight and thermal properties to obtain

derived-lignin chemicals and evaluate potential industrial applications as resins, adhesives, emulsification agents, etc.

REFERENCES

Abbott, A. P, Boothby, D., Capper, G., Davies, D. L., & Rasheed, R. (2004). Deep Eutectic Solvents Formed Between Choline Chloride and Carboxylic Acids. *Journal of American Chemical Society*, *126*(9), 9142–9147.

Abbott, Andrew P., Barron, J. C., Ryder, K. S., & Wilson, D. (2007). Eutectic-based ionic liquids with metal-containing anions and cations. *Chemistry - A European Journal*, *13*(22), 6495–6501. https://doi.org/10.1002/chem.200601738

Abbott, Andrew P., Bell, T. J., Handa, S., Stoddart, B., Data, R. U. S. A., Smith, M. E., … Roberto, I. C. (2006). IIII ‖ United States Patent (19). *Cellulose*, *92*(19), 641–649. https://doi.org/10.1016/j.indcrop.2016.08.003

Abbott, Andrew P., Harris, R. C., Ryder, K. S., D'Agostino, C., Gladden, L. F., & Mantle, M. D. (2011). Glycerol eutectics as sustainable solvent systems. *Green Chemistry*, *13*(1), 82–90. https://doi.org/10.1039/c0gc00395f

Adnan, A. S., Haafiz, M. K. M., Syakir, M. ., Fazita, M. . N., Hossain, M. S., Dungani, R., … Paridah, M. T. (2016). A review on nanocellulosic fibres as new material for sustainable packaging: Process and applications. *Renewable and Sustainable Energy Reviews*, *64*, 823–836. https://doi.org/10.1016/j.rser.2016.06.072

Aguilar-Reynosa, A., Romaní, A., Rodríguez-Jasso, R. M., Aguilar, C. N., Garrote, G., & Ruiz, H. A. (2017). Comparison of microwave and conduction-convection heating autohydrolysis pretreatment for bioethanol production. *Bioresource Technology*, *243*, 273–283. https://doi.org/10.1016/j.biortech.2017.06.096

Alexandre, V. M. F., Mathias, T. R. dos S., Sérvulo, E. F. C., Cammarota, M. C., & de Mello, P. P. M. (2015). Characterization and determination of brewer's solid wastes composition. *Journal of the Institute of Brewing*, *121*(3), 400–404. https://doi.org/10.1002/jib.229

Ambavaram, M. M. R., Krishnan, A., Trijatmiko, K. R., & Pereira, A. (2010). Coordinated Activation of Cellulose and Repression of Lignin Biosynthesis Pathways in Rice. *Plant Physiology*, *155*(2), 916–931. https://doi.org/10.1104/pp.110.168641

American Standard Testing Material. (2003). Standard Test Methods for Direct Moisture Content Measurement of Wood and Wood-Base Materials. *Astm D 4442-92*, *04*(Reapproved 2003), 1–6.

Aquino, G. L. B. de, Signini, R., Bukzem, A. de L., Ascheri, D. P. R., & Santos, D. M. dos. (2015). Microwave-assisted carboxymethylation of cellulose extracted from brewer's spent grain. *Carbohydrate Polymers*, *131*, 125–133. https://doi.org/10.1016/j.carbpol.2015.05.051

ASTM. (2013). Standard Test Method for Preparation of Extractive-Free Wood 1. *Astm*, *96*(Reapproved), 1–2. https://doi.org/10.1520/D1105-96R13.4.2

Baruah, J., Nath, B. K., Sharma, R., Kumar, S., Deka, R. C., Baruah, D. C., & Kalita, E. (2018). Recent Trends in the Pretreatment of Lignocellulosic Biomass for Value-Added Products. *Frontiers in Energy Research*, *6*(December), 1–19. https://doi.org/10.3389/fenrg.2018.00141

Biomedicas, I. (2018). *Porous Sponges from the Mesocarp of Theobroma Cacao L . Fo r P ee r R ev Fo r P r R.*

Bohn, A. (2017). X-ray diffraction as a tool for structural characterization of cellulosic materials. *International Training School on Nanocellulose Characterization*, (January), 17–19.

Brányik, T., Vicente, A. A., Machado Cruz, J. M., Teixeira, J. J. A., Sun, Y., Cheng, J., … Oksman, K. (2019). Bioconversion of brewer's spent grains to bioethanol. *Bioresource Technology*, *8*(3), 1175–1184. https://doi.org/10.1111/j.1567-1364.2008.00390.x

Brown, M. (1999). *Cellulose structure and biosynthesis*. *71*(5), 767–775.

Bubalo, M., Senka Vidovic, S., Redovnikovic, I., & Joki, S. (2018). New perspective in extraction of plant biologically active compounds by green solvents. *Food and Bioproducts Processing*, *9*, 52–73. https://doi.org/10.1016/j.fbp.2018.03.001

Carpita, N. C. (1996). *STRUCTURE AND BIOGENESIS OF THE CELL WALLS OF GRASSES.*

Chakdar, H., Kumar, M., Pandiyan, K., Singh, A., Nanjappan, K., Kashyap, P. L., & Srivastava, A. K. (2016). Bacterial xylanases: biology to biotechnology. *3 Biotech*, *6*(2), 1–15. https://doi.org/10.1007/s13205-016-0457-z

Charpentier, J. C. (2016). What Kind of Modern "green" Chemical Engineering is Required for the Design of the "factory of Future"? *Procedia Engineering*, *138*(0), 445–458. https://doi.org/10.1016/j.proeng.2016.02.104

Chen, Q., Wang, T., Ma, Y., Zhang, Y., Yu, H., Li, J., … Wang, W. (2018). Natural products, an important resource for discovery of
multitarget drugs and functional food for regulation of hepatic glucose metabolism. *Drug Design, Development and Therapy*, *Volume 12*, 121–135. https://doi.org/10.2147/dddt.s151860

Chen, Z., & Wan, C. (2018). Ultrafast fractionation of lignocellulosic biomass by microwave-assisted deep eutectic solvent pretreatment. *Bioresource Technology*, *250*(November 2017), 532–537. https://doi.org/10.1016/j.biortech.2017.11.066

Ciolacu, D., Ciolacu, F., & Popa, V. (2010). Amorphous Cellulose- Structure and Characterization. *Analysis*, *45*, 13–21.

Craveiro, R., Aroso, I., Flammia, V., Carvalho, T., Viciosa, M. T., Dionísio, M., … Paiva, A. (2016). Properties and thermal behavior of natural deep eutectic solvents. *Journal of Molecular Liquids*, *215*, 534–540. https://doi.org/10.1016/j.molliq.2016.01.038

Dai, Y., Spronsen, J. Van, & Witkamp, G. (2013). A Natural deep eutectic solvents as new potential media for green technology. *Analytica Chimica Acta*, *766*, 61–68.

Dai, Y., Verpoorte, R., & Choi, Y. H. (2014). Natural deep eutectic solvents providing enhanced stability of natural colorants from safflower (Carthamus tinctorius). *Food Chemistry*, *159*, 116–121. https://doi.org/10.1016/j.foodchem.2014.02.155

Diels, L. (2019). Bio based Aromatics- Challenges, hurdles and opportunities. *5th Latin American Congress on Biorefineries*.

Domínguez-Domínguez, M. M., Álvarez-Castillo, A., Granados-Baeza, M., & Hernández-Campos, F. (2012). Estudio de la cinética del pretatramiento e hidrólisis ácida del bagazo de caña de azúcar. *Iberoamericana de Polimeros*, *13*(4), 200–211.

Durand, E., Lecomte, J., & Villeneuve, P. (2016). From green chemistry to nature: The versatile role of low transition temperature mixtures. *Biochimie*, *120*, 119–123. https://doi.org/10.1016/j.biochi.2015.09.019

El Comercio. (2016). La bebida alcohólica favorita de los ecuatorianos es la cerveza. Retrieved from https://www.elcomercio.com/tendencias/cerveza-consumo-ecuador-bebidasalcoholicas-historia.html

Elmekawy, A., Diels, L., De Wever, H., & Pant, D. (2013). Valorization of cereal based biorefinery byproducts: Reality and expectations. *Environmental Science and Technology*, *47*(16), 9014–9027. https://doi.org/10.1021/es402395g

Feng, Y. H., Cheng, T. Y., Yang, W. G., Ma, P. T., He, H. Z., Yin, X. C., & Yu, X. X. (2018). Characteristics and environmentally friendly extraction of cellulose nanofibrils from sugarcane bagasse. *Industrial Crops and Products*, *111*(March 2017), 285–291. https://doi.org/10.1016/j.indcrop.2017.10.041

Francisco, M., Van Den Bruinhorst, A., & Kroon, M. C. (2012). New natural and renewable low transition temperature mixtures (LTTMs): Screening as solvents for lignocellulosic biomass processing. *Green Chemistry*, *14*(8), 2153–2157. https://doi.org/10.1039/c2gc35660k

Galia, A., Schiavo, B., Antonetti, C., Galletti, A. M. R., Interrante, L., Lessi, M., … Valenti, M. G. (2015). Autohydrolysis pretreatment of Arundo donax: A comparison between microwave-assisted batch and fast heating rate flow-through reaction systems. *Biotechnology for Biofuels*, *8*(1), 1–19. https://doi.org/10.1186/s13068-015-0398-5

Hassan, S. S., Williams, G. A., & Jaiswal, A. K. (2019). Lignocellulosic Biorefineries in Europe: Current State and Prospects. *Trends in Biotechnology*, *37*(3), 231–234. https://doi.org/10.1016/j.tibtech.2018.07.002

Hideno, A., Inoue, H., Tsukahara, K., Fujimoto, S., Minowa, T., Inoue, S., … Sawayama, S. (2009). Wet disk milling pretreatment without sulfuric acid for enzymatic hydrolysis of rice straw. *Bioresource Technology*, *100*(10), 2706–2711. https://doi.org/10.1016/j.biortech.2008.12.057

ITW Reagents. (2007). *Determination by Kjeldahl Method Nitrogen Determination by Kjeldahl Method*. 1–12. Retrieved from www.itwreagents.com

Jayaramudu, T., Ko, H., Chan, H., Woong, J., Sik, E., & Kim, J. (2019). Adhesion properties of poly (ethylene oxide) -lignin blend for nanocellulose composites. *Composites Part B*, *156*(May 2018), 43–50. https://doi.org/10.1016/j.compositesb.2018.08.063

Kenny, M., Torre, L., & Fortunati, E. (2019). *5.1 Introduction*. https://doi.org/10.1016/B978-0-08-102426-3.00005-9

Khandelwal, S., Tailor, Y. K., & Kumar, M. (2016). Deep eutectic solvents (DESs) as eco-friendly and sustainable solvent/catalyst systems in organic transformations. *Journal of Molecular Liquids*, *215*, 345–386. https://doi.org/10.1016/j.molliq.2015.12.015 Review

Kian, L. K., Jawaid, M., Ariffin, H., & Karim, Z. (2018). Isolation and characterization of nanocrystalline cellulose from roselle-derived microcrystalline cellulose. *International Journal of Biological Macromolecules*, *114*, 54–63. https://doi.org/10.1016/j.ijbiomac.2018.03.065

Klein Marcuschamer, D., Simmons, B. A., & Blanch, H. W. (2011). Techno economic analysis of a lignocellulosic ethanol biorefinery with ionic liquid pre treatment. *Biofuels, Bioproducts and Biorefining*, *5*(5), 562–569.

Kondo, T., Rytczak, P., & Bielecki, S. (2016). Bacterial NanoCellulose Characterization. In *Bacterial Nanocellulose: From Biotechnology to Bio-Economy*. https://doi.org/10.1016/B978-0-444-63458-0.00004-4

Kristiansson, L. (2012). *Chemical Bleaching of Wood and Its Aging : An investigation of Mahogany, Walnut, Rosewood, Padauk and Purpleheart*. *62*(June).

Lee, H., Sundaram, J., Zhu, L., Zhao, Y., & Mani, S. (2018). Improved thermal stability of cellulose nanofibrils using low-concentration alkaline pretreatment. *Carbohydrate Polymers*, *181*(September 2017), 506–513. https://doi.org/10.1016/j.carbpol.2017.08.119

Lei, T., Zeng, X., Liu, S., Li, Z., Sun, Y., Tang, X., … Zuo, M. (2017). Green Processing of Lignocellulosic Biomass and Its Derivatives in Deep Eutectic Solvents. *ChemSusChem*, *10*(13), 2696–2706. https://doi.org/10.1002/cssc.201700457

Li, G., Liu, W., Ye, C., Li, X., & Si, C. L. (2018). Chemocatalytic Conversion of Cellulose into Key Platform Chemicals. *International Journal of Polymer Science*, *2018*. https://doi.org/10.1155/2018/4723573

Li, Z., Yan, J., Shen, D., & Ding, C. (2012). Thecniques and Optimization of Combined Enzymatic Hydrolisis of Brewers´Spent Grain. *Journal of Life Science*, (6), 1232–1236.

Liimatainen, H., Laitinen, O., Li, P., Ojala, J., Selkälä, T., Sirviö, J. A., & Suopajärvi, T. (2016). Deep eutectic solvents in nanocellulose production and functionalization. *7Th Workshop on Cellulose, Regenerated Cellulose and Cellulose Derivatives*, (November).

Lin, N., & Dufresne, A. (2014). Nanocellulose in biomedicine: Current status and future prospect. *European Polymer Journal*, *59*, 302–325. https://doi.org/10.1016/j.eurpolymj.2014.07.025

Lin, O. H., Villagracia, A. R., Mohaiyiddin, M. S., Zakaria, S., Owi, W. T., Chia, C. H., … Md Akil, H. (2016). Comparative Study of Microcelluloses Isolated From Two Different Biomasses with Commercial Cellulose. *BioResources*, *11*(2), 3453–3465. https://doi.org/10.15376/biores.11.2.3453-3465

Loow, Y. L., New, E. K., Yang, G. H., Ang, L. Y., Foo, L. Y. W., & Wu, T. Y. (2017). Potential use of deep eutectic solvents to facilitate lignocellulosic biomass utilization and conversion. *Cellulose*, *24*(9), 3591–3618. https://doi.org/10.1007/s10570-017-1358-y

Lorente, A., Remón, J., Budarin, V. L., Sánchez-verdú, P., Moreno, A., Clark, J. H., … Buchert, J. (2015). Production of oligosaccharides by autohydrolysis of brewery's spent grain.

Carbohydrate Polymers, *92*(3), 324–331. https://doi.org/10.1002/j.2050-0416.2008.tb00774.x

Lynch, K. M., Steffen, E. J., & Arendt, E. K. (2016). Brewers' spent grain: a review with an emphasis on food and health. *Journal of the Institute of Brewing*, *122*(4), 553–568. https://doi.org/10.1002/jib.363

Ma, R., Geleynse, S., Zhang, X., Alvarez-Vasco, C., Guo, M., Ramasamy, K. K., … Wolcott, M. (2016). Unique low-molecular-weight lignin with high purity extracted from wood by deep eutectic solvents (DES): a source of lignin for valorization. *Green Chemistry*, *18*(19), 5133–5141. https://doi.org/10.1039/c6gc01007e

Maehre, H., Dalheim, L., Edvinsen, G., Elvevoll, E., & Jensen, I. (2018). Protein Determination—Method Matters. *Foods*, *7*(2), 5. https://doi.org/10.3390/foods7010005

Mahardika, M., Arief, S., Kasim, A., Abral, H., & Asrofi, M. (2018). Production of Nanocellulose from Pineapple Leaf Fibers via High-Shear Homogenization and Ultrasonication. *Fibers*, *6*(2), 28. https://doi.org/10.3390/fib6020028

Mamilla, J. L. K., Novak, U., Grilc, M., & Likozar, B. (2019). *Biomass and Bioenergy Natural deep eutectic solvents (DES) for fractionation of waste lignocellulosic biomass and its cascade conversion to value-added bio-based chemicals*. *120*(December 2018), 417–425. https://doi.org/10.1016/j.biombioe.2018.12.002

Mandal, A., & Chakrabarty, D. (2011). Isolation of nanocellulose from waste sugarcane bagasse (SCB) and its characterization. *Carbohydrate Polymers*, *86*(3), 1291–1299. https://doi.org/10.1016/j.carbpol.2011.06.030

Marcus, Y. (2018). Deep Eutectic Solvents. *Deep Eutectic Solvents*, *10*(4), 8039–8047. https://doi.org/10.1007/978-3-030-00608-2

Matsutani, A., Harada, T., Ozaki, S., & Takaoka, T. (1993). Inhibitory effects of combination of CDDP and cepharanthin on the cultured cells from rat ascites hepatoma. In *Journal of Japan Society for Cancer Therapy* (Vol. 28).

Meg LaTorre-Snyder. (2017). Lyophilization: The Basics. An overview of the lyophilization process as well as the advantages and disadvantages. *Pharmaceutical Processing*, *32*(1).

Meléndez-Martínez, A. J., Vicario, I. M., & Heredia, F. J. (2007). Review: Analysis of carotenoids in orange juice. *Journal of Food Composition and Analysis*, *20*(7), 638–649. https://doi.org/10.1016/j.jfca.2007.04.006

Meneses, N. G. T., Martins, S., Teixeira, J. A., & Mussatto, S. I. (2013). Influence of extraction solvents on the recovery of antioxidant phenolic compounds from brewer's spent grains. *Separation and Purification Technology*, *108*, 152–158. https://doi.org/10.1016/j.seppur.2013.02.015

Mishra, R. K., Sabu, A., & Tiwari, S. K. (2018). Materials chemistry and the futurist eco-friendly applications of nanocellulose: Status and prospect. *Journal of Saudi Chemical Society*, *22*(8), 949–978. https://doi.org/10.1016/j.jscs.2018.02.005

Mondal, S. (2017). Preparation, properties and applications of nanocellulosic materials. *Carbohydrate Polymers*, *163*, 301–316. https://doi.org/10.1016/j.carbpol.2016.12.050

Moreira, M. M., Morais, S., Barros, A. A., Delerue-Matos, C., & Guido, L. F. (2012). A novel application of microwave-assisted extraction of polyphenols from brewer's spent grain with HPLC-DAD-MS analysis. *Analytical and Bioanalytical Chemistry*, *403*(4), 1019–1029. https://doi.org/10.1007/s00216-011-5703-y

Mussatto, S. I. (2014). Brewer's spent grain: A valuable feedstock for industrial applications. *Journal of the Science of Food and Agriculture*, *94*(7), 1264–1275. https://doi.org/10.1002/jsfa.6486

Mussatto, S. I., & Roberto, I. C. (2005). Acid hydrolysis and fermentation of brewer's spent grain to produce xylitol. *Journal of the Science of Food and Agriculture*, *85*(14), 2453–2460. https://doi.org/10.1002/jsfa.2276

Mussatto, S. I., & Roberto, I. C. (2006). Chemical characterization and liberation of pentose sugars from brewer's spent grain. *Journal of Chemical Technology and Biotechnology*, *81*(3), 268–274. https://doi.org/10.1002/jctb.1374

Naidu, D. S., Hlangothi, S. P., & John, M. J. (2018). Bio-based products from xylan: A review. *Carbohydrate Polymers*, *179*(September 2017), 28–41. https://doi.org/10.1016/j.carbpol.2017.09.064

Orejuela, L., Renneckar, S., Goodell, B., Frazier, C. F., & Edgar, K. J. (2017). *Lignocellulose deconstruction using glyceline and a chelator-mediated Fenton system*.

Palaniappan, A., Yuvaraj, S. S., Sonaimuthu, S., & Antony, U. (2017). Characterization of xylan from rice bran and finger millet seed coat for functional food applications. *Journal of Cereal Science*, *75*, 296–305. https://doi.org/10.1016/j.jcs.2017.03.032

Pan, M., Gan, X., Mei, C., & Liang, Y. (2017). Structural analysis and transformation of

biosilica during lignocellulose fractionation of rice straw. *Journal of Molecular Structure*, *1127*, 575–582. https://doi.org/10.1016/j.molstruc.2016.08.002

Pan, M., Zhao, G., Ding, C., Wu, B., Lian, Z., & Lian, H. (2017). Physicochemical transformation of rice straw after pretreatment with a deep eutectic solvent of choline chloride/urea. *Carbohydrate Polymers*, *176*(August), 307–314. https://doi.org/10.1016/j.carbpol.2017.08.088

Paschos, T., Xiros, C., & Christakopoulos, P. (2015). Simultaneous saccharification and fermentation by co-cultures of Fusarium oxysporum and Saccharomyces cerevisiae enhances ethanol production from liquefied wheat straw at high solid content. *Industrial Crops and Products*, *76*, 793–802. https://doi.org/10.1016/j.indcrop.2015.07.061

Procentese, A., Raganati, F., Olivieri, G., Russo, M. E., Rehmann, L., & Marzocchella, A. (2018). Biotechnology for Biofuels Deep Eutectic Solvents pretreatment of agro industrial food waste. *Biotechnology for Biofuels*, 1–12. https://doi.org/10.1186/s13068-018-1034-y

Radošević, K., Cvjetko Bubalo, M., Gaurina Srček, V., Grgas, D., Landeka Dragičević, T., & Redovniković, R. I. (2015). Evaluation of toxicity and biodegradability of choline chloride based deep eutectic solvents. *Ecotoxicology and Environmental Safety*, *112*(9550), 46–53. https://doi.org/10.1016/j.ecoenv.2014.09.034

Rajendran, K., Drielak, E., Varma, V. S., Muthusamy, S., & Kumar, G. (2017). *Updates on the pretreatment of lignocellulosic feedstocks for bioenergy production – a review*. https://doi.org/10.1007/s13399-017-0269-3

Ralph, J. (1998). *LIGNIN STRUCTURE: RECENT DEVELOPMENTS John Ralph*. (608), 1–16.

Reubroycharoen, P., Phanthong, P., Abudula, A., Hao, X., Xu, G., & Guan, G. (2018). Nanocellulose: Extraction and application. *Carbon Resources Conversion*, *1*(1), 32–43. https://doi.org/10.1016/j.crcon.2018.05.004

Savitha Prashanth, M. R., & Muralikrishna, G. (2014). Arabinoxylan from finger millet (Eleusine coracana, v. Indaf 15) bran: Purification and characterization. *Carbohydrate Polymers*, *99*, 800–807. https://doi.org/10.1016/j.carbpol.2013.08.079

Scheller, H. V., & Ulvskov, P. (2010). Hemicelluloses. *Annual Review of Plant Biology*, *61*(1), 263–289. https://doi.org/10.1146/annurev-arplant-042809-112315

Segal, L., Creely, J. J., Martin, A. E., & Conrad, C. M. (1959). An Empirical Method for

Estimating the Degree of Crystallinity of Native Cellulose Using the X-Ray Diffractometer. *Textile Research Journal*, *29*(10), 786–794. https://doi.org/10.1177/004051755902901003

Singh, R. D., Banerjee, J., Sasmal, S., Muir, J., & Arora, A. (2018). High xylan recovery using two stage alkali pre-treatment process from high lignin biomass and its valorisation to xylooligosaccharides of low degree of polymerisation. *Bioresource Technology*, *256*(December 2017), 110–117. https://doi.org/10.1016/j.biortech.2018.02.009

Singh, V., Parsons, C., & Pettigrew, J. (2007). Distiller's dried grains with solubles. *INFORM - International News on Fats, Oils and Related Materials*, *18*(10), 658–660.

Sluiter, A., Hames, B., Ruiz, R. O., Scarlata, C., Sluiter, J., Templeton, D., … Kreft, J.-U. (2008). Determination of Ash in Biomass, Technical Report NREL/TP-510-42622. *Technical Report NREL/TP-510-42622*, (January). https://doi.org/TP-510-42622

Sun, S. L., Wen, J. L., Ma, M. G., & Sun, R. C. (2013). Successive alkali extraction and structural characterization of hemicelluloses from sweet sorghum stem. *Carbohydrate Polymers*, *92*(2), 2224–2231. https://doi.org/10.1016/j.carbpol.2012.11.098

Sun, Y., Cheng, J., García-Cubero, M. T., Plaza, P., Coca, M., Lucas, S., … Allaf, K. (2016). Synthesis of sugars by hydrolysis of hemicelluloses- A review. *Chemical Reviews*, *83*(1), S88. https://doi.org/10.1186/s13068-015-0398-5

Szymańska-Chargot, M., Chylińska, M., Pieczywek, P. M., & Zdunek, A. (2019). Tailored nanocellulose structure depending on the origin. Example of apple parenchyma and carrot root celluloses. *Carbohydrate Polymers*, *210*(January), 186–195. https://doi.org/10.1016/j.carbpol.2019.01.070

Vigier, K. D. O., Chatel, G., & Jérôme, F. (2015). Contribution of deep eutectic solvents for biomass processing: Opportunities, challenges, and limitations. *ChemCatChem*, *7*(8), 1250–1260. https://doi.org/10.1002/cctc.201500134

Wang, Z., Yao, Z. J., Zhou, J., & Zhang, Y. (2017). Reuse of waste cotton cloth for the extraction of cellulose nanocrystals. *Carbohydrate Polymers*, *157*, 945–952. https://doi.org/10.1016/j.carbpol.2016.10.044

Wertz, Deleu, Coppé, R. (2017). *Hemicelluloses and Lignin in Biorefineries* (1st Editio). https://doi.org/https://doi.org/10.1201/b22136

Wertz, J. L., Deleu, M., Coppée, S., & Richel, A. (2017). Hemicelluloses and lignin in biorefineries. In *Hemicelluloses and Lignin in Biorefineries*. https://doi.org/10.1201/b22136

Wilkinson, S., Smart, K. A., James, S., & Cook, D. J. (2017). Bioethanol Production from Brewers Spent Grains Using a Fungal Consolidated Bioprocessing (CBP) Approach. *Bioenergy Research*, *10*(1), 146–157. https://doi.org/10.1007/s12155-016-9782-7

Wolfson, A., Dlugy, C., Shotland, Y., & Tavor, D. (2009). Glycerol as solvent and hydrogen donor in transfer hydrogenation-dehydrogenation reactions. *Tetrahedron Letters*, *50*(43), 5951–5953. https://doi.org/10.1016/j.tetlet.2009.08.035

Xing, W., Xu, G., Dong, J., Han, R., & Ni, Y. (2018). Novel dihydrogen-bonding deep eutectic solvents: Pretreatment of rice straw for butanol fermentation featuring enzyme recycling and high solvent yield. *Chemical Engineering Journal*, *333*(September 2017), 712–720. https://doi.org/10.1016/j.cej.2017.09.176

Yue, Y. (2011). a Comparative Study of Cellulose I and Ii Fibers and Nanocrystals. *B.S., Heilongjiang Institute of Science and Technology*.

Zhang, C. W., Xia, S. Q., & Ma, P. S. (2016). Facile pretreatment of lignocellulosic biomass using deep eutectic solvents. *Bioresource Technology*, *219*, 1–5. https://doi.org/10.1016/j.biortech.2016.07.026

Zhang, L., Yan, L., Wang, Z., Laskar, D. D., Swita, M. S., Cort, J. R., & Yang, B. (2015). Characterization of lignin derived from water-only and dilute acid flowthrough pretreatment of poplar wood at elevated temperatures. *Biotechnology for Biofuels*, *8*(1), 1–14. https://doi.org/10.1186/s13068-015-0377-x

Zhang, W., Barone, J. R., & Renneckar, S. (2015). Biomass fractionation after denaturing cell walls by glycerol thermal processing. *ACS Sustainable Chemistry and Engineering*, *3*(3), 413–420. https://doi.org/10.1021/sc500564g

Zhang, Z., Harrison, M. D., Rackemann, D. W., Doherty, W. O. S., & O'Hara, I. M. (2016). Organosolv pretreatment of plant biomass for enhanced enzymatic saccharification. *Green Chemistry*, *18*(2), 360–381. https://doi.org/10.1039/c5gc02034d

Zhao, W., Glavas, L., Odelius, K., Edlund, U., & Albertsson, A. C. (2014). A robust pathway to electrically conductive hemicellulose hydrogels with high and controllable swelling behavior. *Polymer*, *55*(13), 2967–2976. https://doi.org/10.1016/j.polymer.2014.05.003

Zhao, X., Cheng, K., & Liu, D. (2009). Organosolv pretreatment of lignocellulosic biomass for enzymatic hydrolysis. *Applied Microbiology and Biotechnology*, *82*(5), 815–827. https://doi.org/10.1007/s00253-009-1883-1

ANNEXES

| **Table 1.** Chemical composition of brewer's spent grain (BSG)										
Component	Kanauchi et al. 2001 *(86)*	Santos et al. 2003 *(7)*	Carvalheiro et al. 2004 *(87)*	Silva et al. 2004 *(88)*	Mussatto and Roberto 2006 *(8)*	Celus et al. 2006 *(16)*	Xiros et al. 2008 *(27)*	Jay et al. 2008 *(89)*	Robertson et al. 2010 *(19)*	Waters et al. 2012 *(9)*	Meneses et al. 2013 *(18)*
Hemicellulose (arabinoxylan)	21.8	n.d.	29.6	41.9	28.4	22.5	40	n.d.	22–29	22.2	19.2
Cellulose	25.4	n.d.	21.9	25.3	16.8	0.3	12	31–33	n.d.	26.0	21.7
Starch	n.d.	n.d.	n.d.		n.d.	1	2.7	10–12	2–8		
Protein	24	31	24.6	n.d.	15.2	26.7	14.2	15–17	20–24	22.1	24.7
Lignin	11.9	16	21.7	16.9	27.8	n.d.	11.5	20–22	13–17	n.d.	19.4
Lipids	10.6	3.0–6.0	n.d.		n.d.	n.d.	13	6–8	n.d.		
Ash	2.4	4.0	1.2	4.6	4.6	3.3	3.3	n.d.	n.d.	1.1	4.2
Phenolics	n.d.	1.7–2.0	n.d.		n.d.	n.d.	2.0	1.0–1.5	0.7–0.9		
All values expressed in g per 100 g dry material (% w/w); n.d., not determined.										

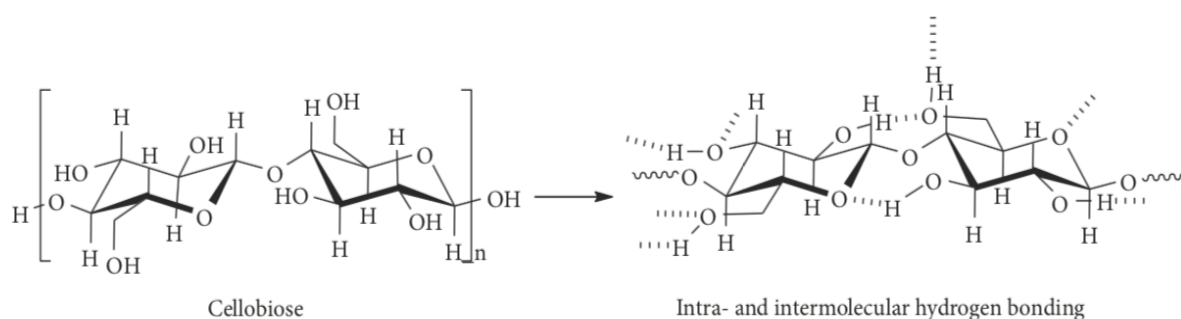**Annex 1.** BSG composition. Taken From (Lynch et al., 2016) under fair use.
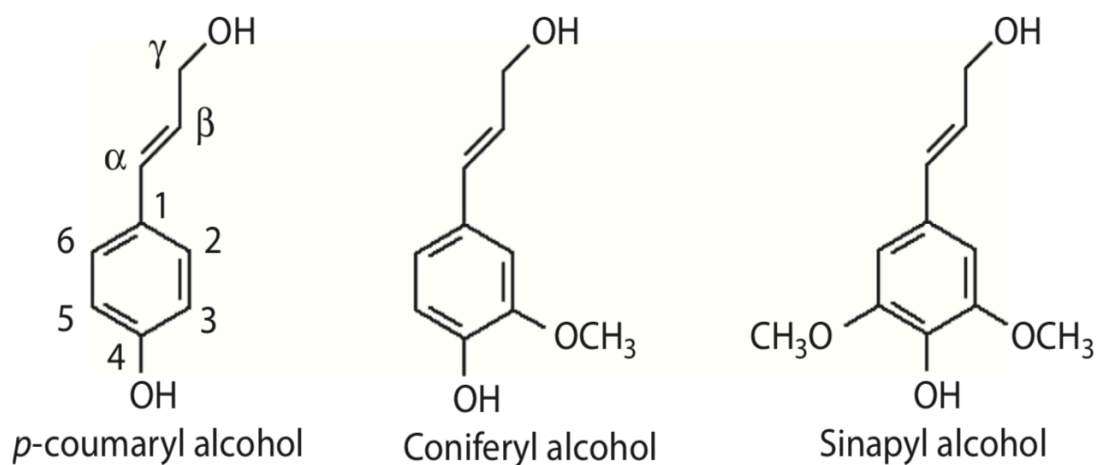
Annex 2. The three main monolignols. Taken from (Wertz, Deleu, Coppé, 2017) under fair use.
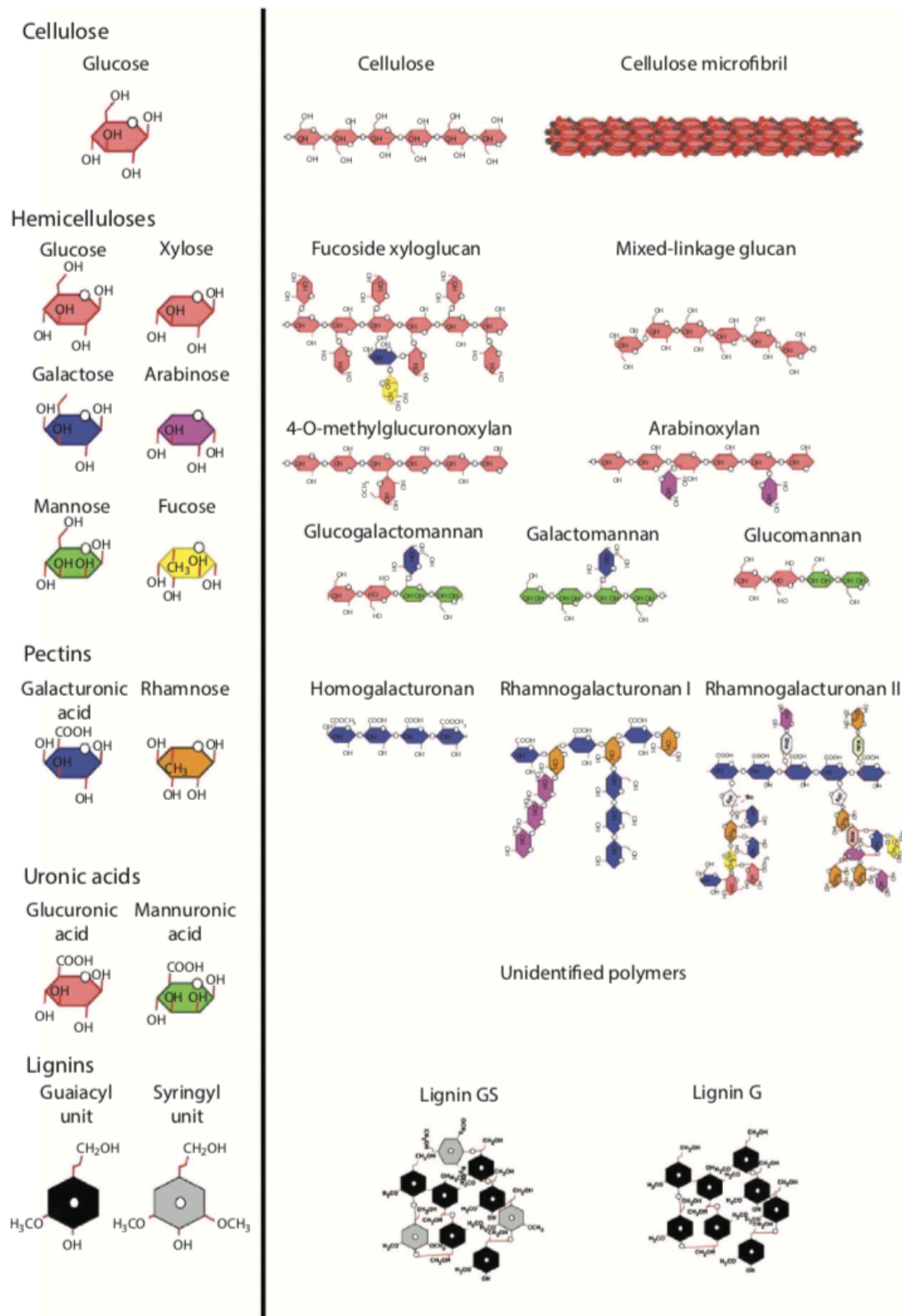
Annex 3. Plant cell wall components. Taken from (Wertz, Deleu, Coppé, 2017) under fair use.
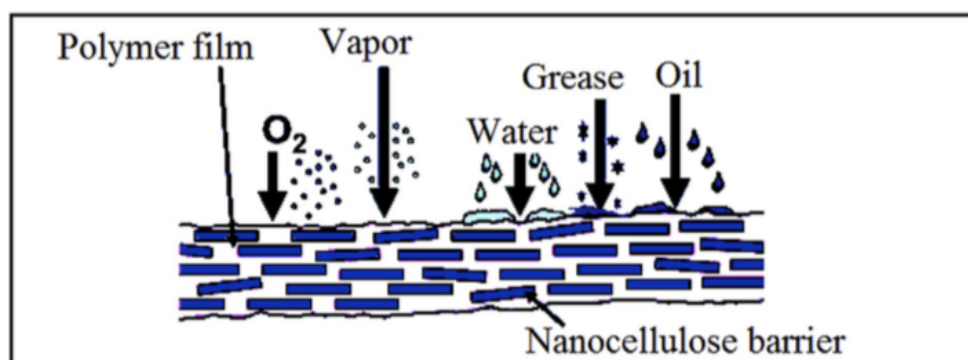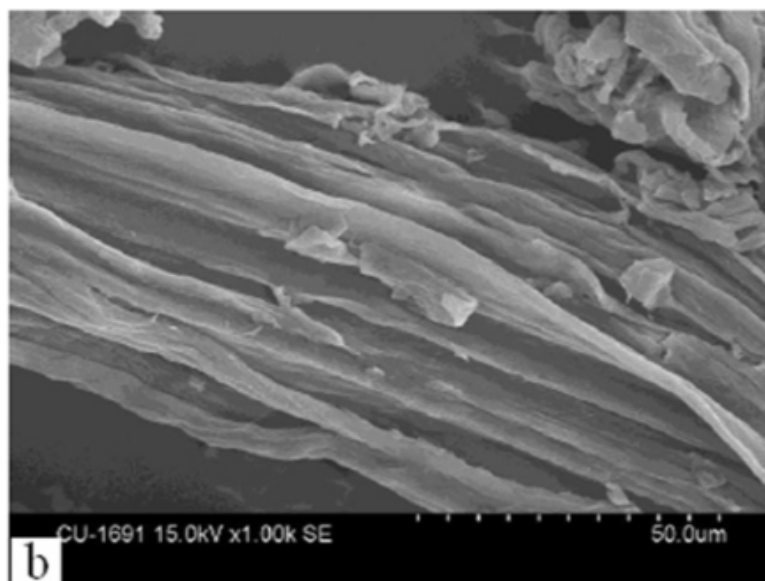
Annex 4. Barrier properties on nanocellulose based films. Taken from (Adnan et al., 2016) under fair use.

SCHEME 1: Chemical structure of cellobiose with β-1,4-glycosidic bonds and intra- and intermolecular hydrogen bonding.

Annex 5. Cellobiose and hydrogen bonding with close by molecules. Taken from (G. Li, Liu, Ye, Li, & Si, 2018) under fair use.

Annex 6. Sugarcane bagasse cellulose. Taken from (G. Li et al., 2018) underfair use.